University of Venda

Numerical analysis of unsteady MHD mixed convection flow past an infinite vertical plate in the presence of Dufour and Soret effects with viscous dissipation

by

Mukwevho Nancy

Supervisor: Prof. S Shateyi

Co-Supervisor: Ms. N.J Netshiozwi

University of Venda

April 9, 2018

Abstract

Magnetohydrodynamics flows have gained significant attention due to their importance in engineering applications. In this study, we numerically analysed the Dufour and Soret effects on an unsteady MHD mixed convection flow past an infinite vertical plate with viscous dissipation. The governing non-linear partial differential equations (PDE_s) are transformed into a system of ordinary differential equations (ODE_s) by the suitable similarity transformations. The resulting equations consist of the momentum, energy and mass diffusion equations. These resulting equations are solved using the Spectral Local Linearization Method (SLLM). Results obtained by the SLLM are in good agreement with the bvp4c technique. The effects of different physical parameters entering into the problem are displayed graphically. The values of the Skin-friction ($f'(0)$), Nusselt number ($-\theta'(0)$) and Sherwood number ($-\phi'(0)$) are shown in tabular form for different values of the parameters. From the results, it is noted that the Soret number (Sr) and the Dufour number (Du) have negligible effects on temperature profile, whereas the decrease in the Soret number (Sr) leads to a decrease in both velocity and concentration of the fluid, and the increase in Dufour number (Du) reduces the velocity and also has negligilbe effect on the concentration profile.

Keywords: Magnetohydrodynamics (MHD), Infinite Vertical Plate, Dufour and Soret effects, Viscous Dissipation, Spectral Local Linearization Method (SLLM).

DECLARATION

I, Mukwevho Nancy, proclaim that this research is my innovative work and has not been submitted for any degree at this or any other university or institution. The research does not embrace other persons writing except where specifically acknowledged and referenced accordingly.

Signature: ..... Date: .....

This work has been submitted for examination with our approval as University supervisors.

ACKNOWLEDGEMENTS

My heartfelt gratitude is extended to the following for their input in the success of this work:

- My supervisor, Prof S. Shateyi for his support and guidance in this journey of my study.
- My co-supervisor, Ms N.J. Netshiozwi for her guidance and advice throughout the study.
- The Department of Mathematics and Applied Mathematics, University of Venda for giving me the opportunity to pursue my dream. The support I got from my colleagues and my fellow students made a huge impact in my study.
- My family, friends and the love of my life, Tsumbedzo Robert Mukwevho for inspiring me throughout this journey.
- My Father in heaven, the Lord Almighty for the gift of life, knowledge and wisdom.

Contents

List of Tables

List of Figures

Nomenclature

b	empirical constant
B_0	uniform magnetic field strength (magnetic induction)
c	suction parameter
C	concentration inside the boundary layer
c_p	specific heat at constant pressure
c_s	concentration susceptibility
C_∞	free stream concentration
Da	Darcy number
Dm	diffusion coefficient
Du	Dufour number
Ec	Eckert number
Fs	Forchheimer number
g	acceleration due to gravity
Gc	Modified Grashof number
Gr	Thermal Grashof number
K	Darcy permeability
k_c	Thermal conductivity of the concentration of the fluid
Kr	chemical reaction parameter
k_T	thermal diffusion ratio
M	Magnetic field parameter
Pr	Prandtl number
q_r	radiative heat flux in the $y-$direction
R	thermal radiation parameter

Re	Local Reynolds number sheet
Sc	Schimdt number
Sr	Soret number
T	thermal temperature inside the thermal boundary layer
T_m	mean fluid temperature
T_∞	free stream temperature
u, v	velocity components along x and $y-$direction respectively
x	flow directional coordinate along the stretching sheet
y	distance normal to the stretching

Greek symbols

θ	non-dimensional temperature parameter
ϕ	non-dimensional concentration parameter
β_t	coefficient of thermal expansion
β_c	coefficient of oncentration expansion
σ	electrical conductivity
ρ	density of the fluid
α	thermal diffusivity
η	similarity variable
ν	kinematic viscosity
μ	Viscosity of the fluid

Index of abbreviations

SLLM	Spectral Local Linearisation Method
ODEs	Ordinary Differential Equations
PDEs	Partial Differential Equations
MHD	Magnetohydrodynamics

Chapter 1

Introduction

In this chapter we outline the background of the study. This chapter will also present literature review for topics related to this study.

1.1 Background

This work deals with the Dufour and Soret effects on an unsteady MHD mixed convection flow past an infinite vertical plate with viscous dissipation.

Magnetohydrodynamics (MHD) flows gained significant attention due to their importance in engineering applications such as geothermal systems, solid matrix heat exchangers, thermal insulations, oil extraction and store of nuclear waste materials.

Dufour and Soret effects are interesting macroscopically as a physical phenomenon in fluid mechanics. When heat and mass transfer occur simultaneously in a moving fluid, affecting each other, this causes cross diffusion effect, the heat transfer caused by concentration gradient is called the diffusion-thermo, which is the Dufour effect and the mass transfer caused by temperature gradient is called thermal diffusion effect, which is the Soret effect.

In a viscous fluid flow the viscosity of the fluid will take energy from the motion of the fluid and transform it into internal energy of the fluid. That means heating up the fluid. This process is partially irreversible and is referred to as viscous dissipation.

1.1.1 Hypothesis

The Dufour and Soret effects with viscous dissipation have impact on the unsteady MHD mixed convection flow passing on an infinite vertical plate.

1.1.2 Purpose of the study

The purpose of this study is to numerically analyse the Dufour and Soret effects with viscous dissipation of the unsteady MHD mixed convection flow past an infinite vertical plate. The numerical method to be used in this study is called the Spectral Local Linearization Method (SLLM).

1.1.3 Research question

The pertinent research question in this study is:

How effective are numerical methods in analysing the unsteady MHD mixed convection flow passing through an infinite vertical plate in the presence of Dufour and Soret effects with viscous dissipation?

1.1.4 Objectives

The study seeks to realise these specific objectives:

- To effectively analyse the unsteady MHD mixed convection flow using a numerical method called Spectral Local Linearisation Method (SLLM).
- To validate the Spectral Local Linearisation Method (SLLM), by comparing the results with those obtained using the MATLAB `bvp4c`.
- To analyse Dufour and Soret effects on an unsteady MHD mixed convection flow passing through an infinite vertical plate.
- To investigate effects of various parameters that affect the fluid flow passing through an infinite vertical plate.

1.1.5 Aims

The aim of this study is to make numerical approximations on the unsteady MHD mixed convection flow, which have been of interest to the engineering community and to the investigators dealing with the problem in geophysics, astrophysics, electrochemistry and polymer processing. The study seeks to see how the unsteady MHD mixed convection flow is affected by the presence of Dufour and Soret effects with viscous dissipation.

1.2 Literature Review

The Dufour and Soret effects are neglected in most studies related to heat and mass transfer, because they are of a smaller order of magnitude compared to the effects described by Fourier's and Fick's laws, but they are important phenomena in areas such as hydrology, petrology and geosciences. The Dufour effect is of considerable magnitude, such that it cannot be neglected. The Soret effect has been utilised for isotope separation and in mixture between gases with very light molecular weight (He, H_2) and of medium molecular weight (N_2, Air).

Some researchers have investigated the Dufour and Soret effects, for example Vempati and Laxmi-Narayana-Gari [46], investigated the Soret and Dufour effects on unsteady MHD flow past an infinite vertical porous plate with thermal radiation. Using the finite element method for the velocity, temperature and concentration field, they concluded that, the velocity increases with an increase of the thermal Grashof number and the solutal Grashof number in the presence of the cooling and heating of the plate, however an increase in the Dufour number leads to an increase in the temperature and an increase in the Soret number leads to an increase in the concentration of the fluid.

Homotopy analysis approach on Dufour and Soret effects on steady MHD convective flow of a fluid in a porous medium with temperature dependent viscosity was presented by Omowaye et al. [30]. The analysis was that, an increase in the Dufour number of the fluid caused a notable reduction in the skin friction coefficient and local heat transfer rate momentarily at the wall of the vertical plate, but increases the magnitude of Sherwood number. An increase in Soret number caused a reduction in skin friction coefficient and

Sherwood number, but increases the magnitude of local heat transfer rate along the flow.

Vedavati et al. [45], studied the radiation and mass transfer effects on unsteady MHD convective flow past an infinite vertical plate with Dufour and Soret effects, employing the shooting method along with Runge-Kutta fourth order integration scheme. From the results they concluded that, heat transfer rate is reduced by increasing thermal radiation parameter and mass transfer rate increases as the Schmidt number increases.

Nalinakshi et al. [29], numerically approached the Soret and Dufour effects on a mixed convection heat and mass transfer with variable fluid properties, using the Shooting technique with Runge-Kutta Fehlberg scheme to obtain velocity, temperature and concentration distribution. Conclusions drawn are that, velocity increases with an increase of Dufour number and decrease of Soret number. As the bouyancy ratio increases, the velocity increases, while temperature and concentration profiles decrease. Rao et al. [32], carried out the finite element analysis of unsteady MHD free convection flow past an infinite vertical plate with Soret, Dufour, thermal radiation and heat source. They used the Galerkin finite element analysis and the results showed that the velocity increases as Grashof number, Dufour number and Soret number increases, However the velocity was found to decrease as the Hartmann number, Prandtl number, Schmidt number, thermal radiation parameter, heat source parameter and Darcy parameter increases.

Soret and Dufour effects on MHD free convection heat and mass transfer flow over a stretching vertical plate with suction and heat source/sink was investigated by Subhakar and Gangadhar [42]. Using Runge-Kutta fourth order method along with Shooting technique they noticed that as the heat generation/absorption parameters increases, the velocity and temperature of the fluid increases, whereas concentration decreases. Gadipally and Gundagani [11], analysed the Soret and Dufour effects on unsteady MHD convective flow past a semi - infinite vertical porous plate using the finite difference method. The results showed that the velocity and temperature profiles increase with an increase of Dufour number throughout the boundary layer and the Schmidt number quantifies the relative effectiveness of momentum and mass transport by diffusion in the hydrodynamic and concentration boundary layers.

The influence of Soret and Dufour effects on MHD free convective heat and mass transfer

flow over a vertical channel with constant suction and viscous dissipation was analysed by Uwanta and Usman [44]. The Implicit Crank-Nicolson method was used and the conclusion was that, concentration profiles decreases due to increase in Schmidt number and suction parameter while it increases due to increase in Soret number and dimensionless time.

The combined influence of Soret and Dufour effects on unsteady hydromagnetic mixed convective flow in an accelerated vertical wavy plate through a porous medium has been investigated by Aruna et al. [5]. Solutions were obtained by applying the finite difference method using symbolic software MATLAB `bvp4c`. Some of the key observations are, the decrease of velocity with an increase in Hartmann number, whereas it increases with an increase in Soret number, Dufour number, porous permeability parameter, thermal Grashof and solutal Grashof numbers.

Dufour and Soret effects on unsteady MHD natural convection flow past vertical plate embedded in non-Darcy porous medium was numerically investigated by Al-Odat and Al-Ghamdi [3]. Using an implicit finite difference scheme of the Crank-Nicolson type with a tridiagonal matrix manipulation, the results showed that, the unsteady velocity, temperature and concentration profiles are substantially influenced by the Dufour and Soret effects. Alam et al. [2], studied numerically the Dufour and Soret effects on unsteady MHD free convection and mass transfer flow past a vertical porous plate in a porous medium. They used Natchtsheim-Swigert shooting iteration technique together with sixth order Runge-Kutta integration scheme. On conclusion, the velocity profiles increase with an increase of Darcy number, also that for fluids with medium molecular weight (H_2, Air), Dufour and Soret effects should not be neglected.

The Soret and Dufour effects on unsteady MHD mixed convection flow past a radiative vertical porous plate embedded in a porous medium with chemical reaction have been studied by Bhupendra et al. [8], results are obtained using an explicit finite-difference scheme. They noticed that suction stabilizes the hydrodynamic, thermal as well as concentration boundary layers growth. Srinivas et al. [41] investigated the effects of thermal-diffusion and diffusion-thermo effects on MHD flow of viscous fluid between expanding or contracting rotating porous disks with viscous dissipation using the analytical ap-

proach called Homotopy analysis method. They noticed that, the results obtained are in good agreement with numerical results obtained by the shooting method coupled with Runge-Kutta scheme.

The Soret and Dufour effects on MHD free convection flow past a vertical porous plate in the presence of heat generation was examined using the fourth order Runge-Kutta method with the shooting technology by Reddy [34]. The conclusions were that, the velocity increase with an increase in Grashof number and modified Grashof number, however, when the Dufour and Soret numbers increases it is seen that the temperature profiles increase.

Osalusi et al. [31] investigated the thermal-diffusion and diffusion-thermo effects on combined heat and mass transfer of a steady MHD convective and slip flow due to a rotating disk with viscous dissipation and ohmic heating. Applying the shooting method, the results showed that, an increase in the value of Dufour number intensifies the effect of Soret number on the concentration profiles, while, an increase in Eckert number at a fixed Dufour number decreases the effect of Soret number on the concentration.

Numerical study of falling film absorption process in a vertical tube absorber including Soret and Dufour effects was conducted by Hosseinnia et al. [12]. Using the finite volume method, they noticed that, including just the inter diffusion term in the energy equation increases the average heat flux at the interface by 8.6% while the average mass flux is reduced by less than 2%, and considering inter-diffusion, Soret and Dufour effects in the governing equations results to higher values of heat and mass flux , around 9.5% and 4%, respectively.

MHD mixed convection flow past a vertical porous plate in a porous medium with heat source/sink and Soret effects was analysed by Kalyani et al. [16], using an implicit finite difference scheme, known as Keller Box method. From the results they drew the conclusion that, the effect of magnetic field parameter is to reduce the velocity profiles, while it increases the temperature and concentration profiles. Both the velocity and concentration profiles increases with the increase of Soret number.

Mondal et al. [24], investigated thermophoresis and Soret-Dufour on MHD mixed convec-

tion mass transfer over an inclined plate with non-uniform heat source/sink and chemical reaction. They numerically solved the equations using Runge-Kutta Fehlberg method with shooting technique. The following conclusions were made: as the thermophoretic parameter increases, there is retardation in the concentration distributions in the boundary layer, however, as the Schmidt number increases, the concentration distribution decreases.

The Soret and Dufour effects on unsteady MHD free convective flow of micropolar fluid with oscillatory plate velocity considering viscous dissipation effects was presented by Shamshuddin and Thirupathi [35]. Using the Galerkin finite element method they concluded that as thermal radiation, Dufour number and viscous dissipation parameter increases, the thickness of thermal boundary layer increases, and an increase in physical parameter causes an increase to thickness of concentration boundary layer while the other parameters reduce the thickness of concentration boundary layer.

A mathematical model is presented by Gangadhar and Suneetha [10], to study the Soret and Dufour effects on MHD free convection flow of a chemically reacting fluid past over a stretching sheet with heat source/sink. Using the fourth order Runge-Kutta method along with shooting technique, it is noticed that the velocity and temperature increases by rising heat generation/absorption parameter, while, the velocity and concentration profiles decrease and temperature profiles increase by rising chemical reaction parameter.

Mohammed and Suneetha [13], studied chemical reaction and Soret effects on unsteady MHD flow of a viscoelastic fluid past an impulsively started infinite vertical plate with heat source/sink. Solving analytically using a regular perturbation technique it was seen that both velocity and concentration profiles decreases with an increase of chemical reaction.

Isah et al. [15], studied the combined effects of thermal diffusion and diffusion thermo effects on transient MHD natural convection and mass transfer flow in a vertical channel with thermal radiation. To verify the accuracy of their results they compared the results obtained analytically by perturbation method with results obtained numerically by semi-implicit finite difference method and the two are in very good agreement. During numerical computation, it was found that the time required reaching steady state velocity

and temperature is directly proportional to the Prandtl number of the working fluid.

Lavanya and Ratnam [17], dealt with the Dufour and Soret effects on steady MHD free convection flow past a vertical porous plate embedded in a porous medium with chemical reaction, radiation, heat generation and viscous dissipation. They used the shooting method along with fourth order Runge-Kutta integration scheme. Comparing the results with previously published work, they reached a good agreement.

Dufour and Soret effects on unsteady free convective flow past a semi-infinite vertical plate with variable viscosity and thermal conductivity was studied by Loganathan et al. [18], using implicit finite difference method of Crank-Nicolson type. An analysis of different parameters shows that, velocity increases with an increase in the Dufour and Soret numbers, temperature decreases with an increase in soret number and concentration profiles increases with an increase of the Soret number but decreases with an increase of the Dufour number.

Suresh et al. [43], numerically investigated an unsteady mixed convective mass and heat transfer MHD flow with Soret effects and viscous dissipation in the presence of thermal radiation and heat source/sink. Using the Matlab ODE-45 solver with shooting method, it was clearly observed that, velocity decreases with increasing of heat source/sink parameter and temperature, whereas, concentration profiles increases by increasing heat source/sink parameter.

Srihari[39], dealt with the effects of radiation and Soret in the presence of heat source/sink on unsteady MHD flow of a chemically reacting fluid with viscous dissipation. Using Crank-Nicolson method, coding in C-programme, it was noticed that skin-friction and Nusselt number increases in the presence of heat source and Eckert number. This is due to the fact that effect of heat generation is to increase the rate of heat transport to the fluid thereby increasing the temperature and velocity of the fluid.

An MHD mixed convection with Soret and Dufour effects past a vertical plate embedded in a porous medium was studied by Makinde[22]. Employing shooting quadrature it was found that the local skin-friction on the plate surface increases with increasing parameter values of E_c, M, S_r, D_u, K and decreases with increasing values of Schmidt number

while the local mass transfer rate at the plate surface increases with increasing values of E_c, M, S_c, D_u, K and decreases with increasing values of Soret number.

The MHD flow and heat transfer problems have become important industrially. Many metallurgical processes involve the cooling of the continuous strips or filaments by drawing them through a quiescent fluid and in the process of drawing, the strips may be stretched. Animasaun [4], studied the dynamics of unsteady MHD convective flow with thermophoresis of particles and variable thermo-physical properties past a vertical surface moving through binary mixture. Employing the shooting technique along with quadratic interpolation scheme, it shows that when variable thermo-physical properties are accounted for transport phenomena of fluid flow along a vertical surface moving through binary mixture in the presence of exponential heat source, Grashof number related to thermal and solutal is an important yard stick to control skin friction drag which arises from the friction of the fluid against the skin of the vertical surface that is moving through binary mixture.

The MHD mixed convection slip flow and heat transfer over a vertical porous plate was presented by Mukhopadhyay and Mandal [28]. Results were obtained numerically using the fourth order classical Runge-Kutta method with the help of shooting method. It was noted that increasing values of suction parameter, the surface temperature decreases. The rate of heat transfer increases with the increased values of velocity slip, magnetic parameter and Prandtl number.

Shateyi and Mabood [36], numerically analyzed the MHD mixed convection slip flow near a stagnation point on a non-linearly vertical stretching sheet in the presence of viscous dissipation using the Runge-Kutta Fehlberg fourth-fifth order method. The results showed clearly that, stretching greatly reduces the skin friction on the wall surface but increases the rate of heat transfer. However, the rate of heat transfer increases as the values of the injection parameter increases.

The MHD mixed convection from a vertical plate embedded in a porous medium with a convective boundary conditions was studied by Makinde and Aziz [23], applying shooting iteration together with a sixth order Runge-Kutta integration algorithm. Their results revealed that both the fluid velocity and temperature increases with an increase in the

convective heat transfer parameter. MHD mixed convection flow, heat and mass transfer of a micropolar fluid over an unsteady stretching sheet with viscous dissipation and thermal radiation was numerically approached by Shateyi and Mabood [37]. Dissipation effect on MHD mixed convection flow over a stretching sheet through porous medium with non-uniform heat source/sink has been investigated by Bhukta et al. [7]. The investigation was numerically done using Runge-Kutta fourth order method associated with shooting technique. From the results they noticed that thinning of thermal boundary layer is affected by heavier diffusing species and it occurs under the influence of increasing wall concentration and variable viscosity.

Rashidi et al. [33], presented the mixed convective heat transfer for MHD viscoelastic fluid flow over a porous wedge with thermal radiation, using the semi-analytical technique known as Homotopy analysis method. The results showed that, as the wedge angle increases the heat transfer to the fluid increases and the magnetic field has a weak effect on the thermal boundary thickness, however, the suction has a remarkable effect on it.

Effects of chemical reaction, heat and mass transfer and viscous dissipation over MHD flow in a vertical porous wall using perturbation method were presented by Ahmed et al. [1]. They outlined important conclusions of their study and some of them are that: the presence of field magnetic will inhabit the fluid motion in view of the decrease of the momentum boundary layer thickness. The temperature of the fliud increase with the decrease of the gradient at the wall. The thickness of the thermal boundary layer causes the decrease of heat transfer from the wall to the fluid.

Srinivasa et al [40], carried out both analytical and numerical study of unsteady MHD free convection flow over an exponentially moving vertical plate with heat absorption. They used the element free Galerkin method as well as the Laplace transformation technique. The conclusion was that, the numerical solutions are in good agreement with the analytical solutions. The numerical solutions are unique for various mesh size at $t = 1.0$, hence the EFMG is stable and it is a suitable numerical method to solve the considered type of model.

A mathematical model developed by Mabood et al. [19] to study the viscous dissipation effects on unsteady mixed convective stagnation point flow using Tiwari-Das nanofluid

model. Applying the Runge-Kutta Fehlberg method with shooting technique, they noticed that velocity rises as nano particle volume fraction (ϕ), magnetic parameter (M), wall transpiration parameter (v_w), mixed convection parameter (λ), unsteadiness parameter (A), velocity ratio parameter (ε) and Eckert number (E_c). However, temperature decreases with unsteadiness parameter (A) and magnetic parameter (M). Skin friction coefficient increases with the increase of nano particle volume fraction (ϕ), wall transpiration parameter (v_w) and Eckert number (E_c).

MHD mixed convective flow past a vertical plate embedded in a porous medium with radiation effects and convective boundary condition considering chemical reaction was examined by Sadeq and Sayyed [47]. They applied an implicit finite difference scheme and the results demonstrated that the values of velocity and temperature are enhanced with increasing the Biot number and the values of concentration are affected by chemical reaction and decrease with increasing the reaction rate parameter. Mahender and Srikanth [21], investigated the unsteady MHD free convection and mass transfer flow past a porous vertical plate in the presence of viscous dissipation. Using a finite element technique, the effects of various parameters were analysed and the results conclude that as magnetic parameter increases the value of velocity decreases. It was also noticed that there is a rise in the temperature and the velocity due to the heat created by the viscous dissipation, free convection and heat source.

In view of the above studies, we notice that most of the works are similar to the problem considered in this work. However, in this present work we are considering the Dufour and Soret effects with viscous dissipation and we will be using the numerical method called the Spectral Local Linearization Method (SLLM). The method was proposed by Motsa [26] for non-linear boundary layer flow problems.

1.3 Definitions of keywords

Numerical Analysis

Numerical analysis is the area of mathematics and computer science that creates, analyzes, and implements algorithms for solving the problems of continuous mathemat-

ics. Such problems originate generally from real-world applications of algebra, geometry and calculus, and they involve variables which vary continuously, these problems occur throughout the natural sciences, social sciences, engineering, medicine, and business. Most mathematical models used in the natural sciences and engineering are based on ordinary differential equations, partial differential equations, and integral equations. The numerical methods for these equations are primarily of two types. The first type approximates the unknown function in the equation by a simpler function, often a polynomial or piecewise polynomial function, choosing it to satisfy the original equation approximately. Among the best known of such methods is the finite element method and finite difference methods, Kendall E. Atkinson [6].

In this study we are using the spectral local linearization method, to numerically analyse our problem.

Magnetohydrodynamic (MHD)

Magneto-fluid dynamics or Magnetohydrodynamics is the study of the magnetic properties of electrically conducting fluids. Examples of such magneto-fluids include plasmas, liquid metals, salt water and electrolytes.

The fundamental concept behind MHD is that magnetic fields can induce currents in a moving conductive fluid, which in turn polarizes the fluid and reciprocally changes the magnetic field itself. The set of equations that describe MHD are a combination of the Navier-Stokes equations of fluid dynamics and Maxwell's equations of electromagnetism. These differential equations must be solved simultaneously, either analytically or numerically [49].

Unsteady Flow

If at any point in the fluid, the conditions change with time, the flow is described as unsteady [48].

Dufour Effect

When heat and mass transfer occur simultaneously in a moving fluid affecting each other, it causes a cross diffusion effect, the heat transfer caused by concentration gradient is called the diffusion-thermo, which is the Dufour effect.

Soret Effect

When heat and mass transfer occur simultaneously in a moving fluid affecting each other, causing cross diffusion effect, the mass transfer caused by temperature gradient is called thermal diffusion effect, which is the Soret effect.

Viscous Dissipation

Viscous dissipation is the irreversible process by means of which the work done by a fluid on adjacent layers due to the action of shear forces is transformed into heat. In a viscous fluid flow the viscosity of the fluid will take the energy from the motion of the fluid (kinetic energy) and transform it into internal energy of the fluid, that is, heating up the fluid.

Chapter 2

Problem Formulation

The equations governing the MHD mixed convection flow of an incompressible and electrically conducting viscous fluid along an infinite vertical plate are derived in this chapter. Additionally, in this chapter the overview of similarity technique will be outlined and the boundary-layer equations will be transformed into ordinary differential equations.

2.1 Derivations of Equations

In this section we will outline the derivations of the governing boundary-layer partial differential equations.

2.1.1 Derivation of continuity equation

The continuity equation is also known as the conservation of mass equation. This is one of the fundamental principles used in the analysis of uniform fluid flow. In this section the partial differential equation will be derived and the derivation will be referred to the work in [50].

Consider fluid mass fixed in an arbitrary region $R(t)$. This region can be identified with a fluid element but in some cases we can choose to associate this with a macroscopic domain. The boundary $S(t)$ of $R(t)$ can generally move with time in either cases. Such region is often called a system in thermodynamics contexts and it can be closed or open. Following [50], it is only important that mass is fixed. For our purpose, it is convenient

to relate the mass of the system to the density of the fluid,

$$m = \int_{R(t)} \rho dV. \tag{2.1}$$

where $R(t)$ and ρ may change with time, but m must be left unchanged in order to have conservation of mass. Mathematical expression is as follows:

$$\frac{dm}{dt} = \frac{d}{dt} \int_{R(t)} \rho dV = 0. \tag{2.2}$$

that is, conservation of mass means that the time rate of change of mass of a system must be zero. In order to obtain a differentiation equation of mass conservation, we apply the general transport theorem to get:

$$\int_{R(t)} \frac{\partial \rho}{\partial t} dV + \int_{S(t)} \rho W.\vec{n} dA = 0. \tag{2.3}$$

It is useful in a fluid system to take the velocity field W to be that of the flowing fluid, which corresponds to locally viewing $R(t)$ as an arbitrary fluid element. Therefore , equation (2.3) becomes:

$$\int_{R(t)} \frac{\partial \rho}{\partial t} dV + \int_{S(t)} \rho U.\vec{n} dA = 0. \tag{2.4}$$

The surface integral must be converted into a volume integral by means of Gauss's theorem, $\int_{S(t)} \rho U.\vec{n} dA = \int_{R(t)} \nabla.\rho U dV$, substituting this into equation (2.4), we get:

$$\int_{R(t)} \left[\frac{\partial \rho}{\partial t} + \nabla.\rho U \right] dV = 0. \tag{2.5}$$

Since the region $R(t)$ was arbitrary, the integrand will be zero within $R(t)$, therefore:

$$\frac{\partial \rho}{\partial t} + \nabla.\rho U = 0. \tag{2.6}$$

Since we are considering an incompressible fluid, $\rho =$ constant, it is independent of space and time, then $\frac{\partial \rho}{\partial t} = 0$. The continuity equation reduces to

$$\nabla.U = 0. \tag{2.7}$$

where $U = \vec{j}y$, since the physical variables are functions of y and t. Therefore continuity equation is given as:

$$\frac{\partial v}{\partial y} = 0. \tag{2.8}$$

2.1.2 Derivation of momentum equation

This derivation is referred to [50]. Newton's second law states that, in an inertial reference frame the time rate of momentum change of a fixed mass system is equal to the net force acting on the system, and it takes place in the direction of the net force. Mathematically this can be written as:

$$\sum F = \frac{d(mV)}{dt}, \tag{2.9}$$

at a constant velocity V, where $\sum F$ is the net force vector acting on the fixed mass system and $\left(\frac{d(mV)}{dt}\right)$ is the rate of change of momentum. From the transformation formula we have the integral form of Newton's second law for control volumes that contains only one phase and it can be obtained by using the following equation:

$$\frac{d\Phi}{dt}|_{system} = \frac{\partial}{\partial t}\int_V \rho\phi dV + \int_A \rho(V.\vec{n})\phi dA, \tag{2.10}$$

where $\Phi = mV$ and $\phi = V$, therefore,

$$\sum F = \frac{\partial}{\partial t}\int_V \rho V dV + \int_A \rho(V.\vec{n})V dA, \tag{2.11}$$

in vector form and it is valid in three directions. Forces acting on the control volume are body forces and contact forces that act on its surface. Therefore the net force is as follows:

$$\sum F = \int_V \left[\sum_{i=1}^{N} \rho_i X_i\right] dV + \int_A \tau'.\vec{n} dA, \tag{2.12}$$

where τ' is the total stress tensor and n is the local normal unit vector on surface A. We then equate equation (2.11) and equation (2.12) to get the integral form of the momentum equation for the control volume of a single phase as:

$$\frac{\partial}{\partial t}\int_V \rho V dV + \int_A \rho(V.\vec{n})V dA = \int_V \left[\sum_{i=1}^{N} \rho_i X_i\right] dV + \int_A \tau'.\vec{n} dA. \tag{2.13}$$

From the above equation the surface integral terms can be written using the divergence theorem: $\int_A \tau'.\vec{n} dA = \int_V \nabla.\tau' dV$ and $\int_A \rho(V.\vec{n})V dA = \int_V [\nabla.\rho V] V dV$, therefore substituting the divergence theorem into the integral momentum equation, we then have:

$$\int_V \left[\nabla.\tau' + \sum_{i=1}^{N} \rho_i X_i - \frac{\partial}{\partial t}(\rho V) - \nabla.\rho VV\right] dV = 0, \tag{2.14}$$

written as a volume integral. The integrand must be zero to validate equation (2.14). Therefore the momentum equation in differential form will be:

$$\frac{\partial}{\partial t}(\rho V) + [\nabla.\rho V]\, V = \nabla.\tau' + \sum_{i=1}^{N} \rho_i X_i. \tag{2.15}$$

Simplifying the derivatives on the left-hand side, we have,

$$V\left[\frac{\partial \rho}{\partial t} + \nabla.\rho V\right] + \rho\left[\frac{\partial V}{\partial t} + V.\nabla V\right] = \nabla.\tau' + \sum_{i=1}^{N} \rho_i X_i. \tag{2.16}$$

By the continuity equation the first bracketed term on the left vanishes and the second bracketed term can be written in substantial derivative form then equation (2.16) will be,

$$\rho\frac{DV}{Dt} = \nabla.\tau' + \sum_{i=1}^{N} \rho_i X_i, \tag{2.17}$$

where the stress tensor $\tau' = -PI + \tau$, so that equation (2.17) becomes:

$$\rho\frac{DV}{Dt} = -\nabla P + \nabla.\tau + \sum_{i=1}^{N} \rho_i X_i. \tag{2.18}$$

By Newton's law of viscosity, $\tau = 2\mu D - \frac{2}{3}\mu(\nabla.V)I$, where D is the rate of strain tensor $D = \frac{1}{2}[\nabla V + (\nabla V)^T]$. Since the fluid is incompressible, ρ = constant and from the continuity equation $\nabla V = 0$, the momentum equation becomes:

$$\rho\frac{DV}{Dt} = \sum_{i=1}^{N} \rho_i X_i - \nabla P + \nabla.(\mu\nabla V). \tag{2.19}$$

The vector form of the momentum equation can be written as three equations in the X, Y and Z directions in a cartesian coordinate system:

$$\rho\frac{DV}{Dt} = \sum_{i=1}^{N} \rho_i X_i - \frac{\partial P}{\partial x} + \mu\left(\frac{\partial^2 u}{\partial x^2} + \frac{\partial^2 u}{\partial y^2} + \frac{\partial^2 u}{\partial z^2}\right), \tag{2.20}$$

$$\rho\frac{DV}{Dt} = \sum_{i=1}^{N} \rho_i Y_i - \frac{\partial P}{\partial y} + \mu\left(\frac{\partial^2 v}{\partial x^2} + \frac{\partial^2 v}{\partial y^2} + \frac{\partial^2 v}{\partial z^2}\right), \tag{2.21}$$

$$\rho\frac{DV}{Dt} = \sum_{i=1}^{N} \rho_i Z_i - \frac{\partial P}{\partial z} + \mu\left(\frac{\partial^2 w}{\partial x^2} + \frac{\partial^2 w}{\partial y^2} + \frac{\partial^2 w}{\partial z^2}\right), \tag{2.22}$$

where X_i, Y_i and Z_i are components of body force per unit volume acting on the i_{th} in the x, y and z directions respectively. The body force is gravity then $X_i = g$, so that equation (2.19) becomes:

$$\rho\frac{DV}{Dt} = \rho g - \nabla P + \nabla.(\mu\nabla V). \tag{2.23}$$

The density of a mixture is a function of temperature and concentration fractions of species. It can be expanded to, as referred from [45],

$$\bar{\rho} = -\frac{\partial\rho}{\partial T}(T - T_\infty) - \frac{\partial\rho}{\partial C}(C - C_\infty) = -\bar{\rho}\beta_t(T - T_\infty) - \bar{\rho}\beta_c(C - C_\infty), \tag{2.24}$$

where $\beta_t = -\frac{\frac{\partial\rho}{\partial T}}{\bar{\rho}}$ is the coefficient of thermal expansion and $\beta_t = -\frac{\frac{\partial\rho}{\partial C}}{\bar{\rho}}$ is the concentration expansion. Substituting equation (2.24) into equation (2.23) we get:

$$\rho\frac{DV}{Dt} = \rho g - \nabla P + \rho g\beta_t(T - T_\infty) + \rho g\beta_c(C - C_\infty) + \nabla.(\mu\nabla V). \tag{2.25}$$

Following, Vedavati et al. [45], terms ρg and $-\nabla P$ are ignored then we have

$$\rho\frac{DV}{Dt} = \nabla.(\mu\nabla V) + \rho g\beta_t(T - T_\infty) + \rho g\beta_c(C - C_\infty). \tag{2.26}$$

The dynamic viscosity $\mu = \gamma\rho$ and considering the X- component and taking the physical variables as functions of y and t only, we have:

$$\rho\frac{DU}{Dt} = \gamma\rho\frac{\partial^2 u}{\partial y^2} + \rho g\beta_t(T - T_\infty) + \rho g\beta_c(C - C_\infty), \tag{2.27}$$

dividing eq (2.27) by ρ, we get:

$$\frac{DU}{Dt} = \gamma\frac{\partial^2 u}{\partial y^2} + g\beta_t(T - T_\infty) + g\beta_c(C - C_\infty). \tag{2.28}$$

Since magnetic field is transversally to the direction of the flow and adding the permeability and empirical terms, we then have the momentum equation as:

$$\begin{aligned}\frac{\partial u}{\partial t} + v\frac{\partial u}{\partial y} = \nu\frac{\partial^2 u}{\partial y^2} + g\beta_t(T - T_\infty) + \\ g\beta_c(C - C_\infty) - \frac{\sigma B_0^2}{\rho}u - \frac{\nu}{K}u - \frac{b}{K}u^2.\end{aligned} \tag{2.29}$$

2.1.3 Derivation of energy equation

This derivation is also referred to [50]. The first law of thermodynamics for closed system states that

$$\left.\frac{dE}{dt}\right|_{system} = \frac{\delta Q}{dt} - \frac{\delta W}{dt}, \tag{2.30}$$

where Q is positive when heat is transferred into the system and W is positive when the work is done by the system. Energy can be stored in different forms in the mass of the system. For this equation we consider the contribution of internal and kinetic energies. The energy equation for the control volume can be obtained from the general property: $\Phi = E + mV^2/2 + mgz$ and $\phi = e + V^2/2 + gz$ being set in,

$$\left.\frac{d\Phi}{dt}\right|_{system} = \frac{\partial}{\partial t}\int_V \rho\phi dV + \int_A \rho(V.\vec{n})\phi dA, \tag{2.31}$$

That is,

$$\left.\frac{dE}{dt}\right|_{system} = \frac{\partial}{\partial t}\int_V \rho(e + \frac{V^2}{2} + gz)dV - \int_A (V.\vec{n})(e + \frac{V^2}{2} + gz)dA, \tag{2.32}$$

where E and e are internal and specific internal energy, respectively. We substitute equation (2.32) into equation (2.30) to get the integral form of the energy equation as:

$$\frac{\delta Q}{dt} - \frac{\delta W}{dt} = \frac{\partial}{\partial t}\int_V \rho(e + \frac{V^2}{2} + gz)dV - \int_A (V.\vec{n})(e + \frac{V^2}{2} + gz)dA, \tag{2.33}$$

where $\frac{\delta Q}{dt} = \int_A -q''.\vec{n}dA + \int_V q'''dV$, where q'' is the heat flux at the control volume surface and is indicated by Fourier's law $q'' = -K.\nabla T$ and q''' is the internal heat generation per unit volume. Work rate term, includes four types of work and can be expressed as:

$$\frac{\delta W}{dt} = \frac{\delta W_{sh}}{dt} + \frac{\delta W_b}{dt} + \frac{\delta W_p}{dt} + \frac{\delta W_s}{dt}, \tag{2.34}$$

where

$$\frac{\delta W_b}{dt} = -\int_V \left[\sum_{i=1}^{N} \rho_i X_i\right], \tag{2.35}$$

$$\frac{\delta W_p}{dt} = -\int_A \rho(V.\vec{n}).dA, \tag{2.36}$$

and

$$\frac{\delta W_s}{dt} = -\int_A (\vec{n}.\tau).V dA. \tag{2.37}$$

Substituting equation (2.34) and equation (2.36) into equation (2.33), we get:

$$\frac{\delta Q}{dt} - \frac{\delta W_{sh}}{dt} - \frac{\delta W_b}{dt} - \frac{\delta W_s}{dt} = \frac{\partial}{\partial t}\int_V \rho(e + \frac{V^2}{2} + gz)dV + \int_A \rho(V.\vec{n})(e + \frac{V^2}{2} + \frac{p}{\rho} + gz)dA. \tag{2.38}$$

The shaft force $\frac{\delta W_{sh}}{dt}$ is neglected for a single phase system and the pressure work is included as part of τ', then the integral energy equation can be written as:

$$\frac{\partial}{dt}\int_V \rho(e + \frac{V^2}{2})dV + \int_A \rho(V.\vec{n})(e + \frac{V^2}{2})dA = -\int_A q''.\vec{n}dA + \int_V q'''dV + \int_A (\vec{n}.\tau').V dA + \int_V \left[\sum_{i=1}^{N} \rho_i X_i\right]. \tag{2.39}$$

Using $\int_A \Omega.\vec{n}dA = \int_V \nabla.\Omega dV$, we can write the above equation as a volume integral. From the transformation formula we have:

$$\int_A \rho(V.\vec{n})(e + \frac{V^2}{2})dA = \int_V \nabla.[\rho V(e + \frac{V^2}{2})]dV, \tag{2.40}$$

$$\int_A -q''.\vec{n}dA = \int_V -\nabla.q''dV, \tag{2.41}$$

$$\int_A \vec{n}.\tau'.V dA = \int_V \nabla.(\tau' V)dV. \tag{2.42}$$

Substituting equations (2.40) - (2.42) into equation (2.39) and considering

$$\frac{d}{dt}\int_V \rho\phi dV = \int_V \frac{\partial(\rho\phi)}{\partial t}dV, \tag{2.43}$$

we get:

$$\int_V \left[\frac{\partial}{\partial t}\left(\rho\left(e + \frac{V^2}{2}\right)\right) + \nabla.\left[\rho V\left(e + \frac{V^2}{2}\right)\right] + \nabla.q'' - q''' - \nabla.(\tau'.V) - \left(\sum_{i=1}^{N} \rho_i X_i\right).V\right]dV = 0. \tag{2.44}$$

The integrand must be zero for equation(2.44) to be valid for an arbitrary control volume, therefore general differential energy equation is given by:

$$\frac{\partial}{\partial t}\left(\rho\left(e+\frac{V^2}{2}\right)\right)+\nabla.\left[\rho V\left(e+\frac{V^2}{2}\right)\right]=-\nabla.q''+q'''+ \nabla.(\tau'.V)+\left(\sum_{i=1}^{N}\rho_i X_i\right).V. \tag{2.45}$$

Expanding equation (2.45), we have,

$$\left(e+\frac{V^2}{2}\right)\left[\frac{\partial\rho}{\partial t}+\nabla.(\rho V)\right]+ \rho\left[\frac{\partial}{\partial t}\left(e+\frac{V^2}{2}\right)+V.\nabla\left(e+\frac{V^2}{2}\right)\right]= -\nabla.q''+q'''+\nabla.(\tau'.V)+\left(\sum_{i=1}^{N}\rho_i X_i\right).V, \tag{2.46}$$

$\frac{\partial\rho}{\partial t}+\nabla.\rho V=0$ from continuity equation and writing the equation in substantial derivative form, that is the total energy balance equation as:

$$\rho\frac{D}{Dt}\left(e+\frac{V^2}{2}\right)=-\nabla.q''+q'''+\nabla.(\tau'.V)+\left(\sum_{i=1}^{N}\rho_i X_i\right).V. \tag{2.47}$$

Removing the mechanical energy term from equation (2.47), we form the dot product of the momentum equation $\rho\frac{DV}{Dt}=\nabla.\tau'+\sum_{i=1}^{N}\rho_i X_i$, from the momentum equation with velocity V, that is:

$$\rho\frac{DV}{Dt}.V=(-\nabla.\tau').V+\left(\sum_{i=1}^{N}\rho_i X_i\right).V. \tag{2.48}$$

Rearranging equation (2.48) we have:

$$\rho\frac{D}{Dt}\left(\frac{V^2}{2}\right)=\nabla.(\tau'.V)+\nabla V:\tau+\left(\sum_{i=1}^{N}\rho_i X_i\right).V. \tag{2.49}$$

Where $\nabla V:\tau$ is the field extension. We subtract equation (2.49) from equation (2.47), to obtain the thermal energy equation:

$$\rho\frac{De}{Dt}=-\nabla.q''+q'''-p\nabla.V+\nabla V:\tau. \tag{2.50}$$

To obtain an equation containing the enthalpy, we use the enthalpy definition: $h=e+\frac{p}{\rho}$, substituting this definition into equation (2.50) and taking note of the continuity equation,

$\frac{\partial \rho}{\partial t} + \nabla . \rho V = 0$, we obtain:

$$\rho \frac{Dh}{Dt} = -\nabla . q'' + \frac{Dp}{Dt} + q''' + \nabla V : \tau, \tag{2.51}$$

which is now the energy equation in terms of enthalpy and temperature. Substituting the heat flux $q'' = -K.\nabla T$, we obtian the following energy equation for a pure substance:

$$\rho \frac{Dh}{Dt} = \nabla . (K \nabla T) + \frac{Dp}{Dt} + q''' + \nabla V : \tau. \tag{2.52}$$

The enthalpy of a pure substance can be expressed as:

$$\frac{Dh}{Dt} = \left(\frac{\partial h}{\partial T} \right)_p \frac{DT}{Dt} + \left(\frac{\partial h}{\partial p} \right)_T \frac{Dp}{Dt}. \tag{2.53}$$

Thermodynamics relations gives: $\left(\frac{\partial h}{\partial T}\right)_p = c_p$ and $\left(\frac{\partial h}{\partial p}\right) = \frac{1-\beta t}{\rho}$, where $\beta = \frac{1}{\rho}\left(\frac{\partial \rho}{\partial T}\right)$ is the thermal expansion coefficient. Then equation (2.53) becomes:

$$\frac{Dh}{Dt} = c_p \frac{DT}{Dt} + \frac{1 - \beta t}{\rho} \frac{Dp}{Dt}. \tag{2.54}$$

Substituting equation (2.54) into equation (2.52), energy equation is given by:

$$\rho c_p \frac{DT}{Dt} = \nabla . (K \nabla T) + T \beta \frac{Dp}{Dt} + q''' + \nabla V : \tau. \tag{2.55}$$

For incompressible fluids, the constant density $\beta = 0$ and the energy equation becomes:

$$\rho c_p \frac{DT}{Dt} = \nabla . (K \nabla T) + q''' + \nabla V : \tau, \tag{2.56}$$

which can be simplified as:

$$\rho c_p \frac{DT}{Dt} = K \left(\frac{\partial^2 T}{\partial y^2} \right) + \frac{\partial q_r}{\partial y} + \frac{\partial u}{\partial y} \left(\mu \frac{\partial u}{\partial y} \right), \tag{2.57}$$

where $\tau = \mu \frac{\partial u}{\partial y}$ and $q''' = \frac{\partial q_r}{\partial y}$.

Dividing both sides of equation (2.57) by ρc_p, we get:

$$\frac{DT}{Dt} = \alpha \frac{\partial^2 T}{\partial y^2} + \frac{1}{\rho c_p} \frac{\partial q_r}{\partial y} + \left(\frac{\partial u}{\partial y} \right)^2 \frac{\mu}{\rho c_p}, \tag{2.58}$$

where $\alpha = \frac{K}{\rho c_p}$. For the current study we add the term for diffusion on concentration which is $\frac{D_m k_T}{c_s c_p} \frac{\partial^2 C}{\partial y^2}$, then our energy equation will be:

$$\frac{\partial T}{\partial t} + v \frac{\partial T}{\partial y} = \alpha \frac{\partial^2 T}{\partial y^2} - \frac{1}{\rho c_p} \frac{\partial q_r}{\partial y} + \frac{D_m k_T}{c_s c_p} \frac{\partial^2 C}{\partial y^2} + \frac{\mu}{\rho c_p} \left(\frac{\partial u}{\partial y} \right)^2. \tag{2.59}$$

2.1.4 Derivation of mass diffusion equation

The mass diffusion equation gives the relationship between addition and removal of the mass from a defined region of fluid. The total mass within the control volume is:

$$M = \int_V C dV, \tag{2.60}$$

where M can change over time, i.e. $M = M(t)$. In a fluid system we have two forms of mass flux, advection and diffusion. Therefore , the net flux mass out of the control volume due to advection is:

$$\int_S C\bar{V}.\bar{n}dA, \tag{2.61}$$

and the net flux mass out of the control volume due to diffusion is defined using Fick's law that is:

$$-\int_S D_n \frac{\partial C}{\partial n} dA. \tag{2.62}$$

Combining equation (2.61) and equation (2.62), we obtain the expression for conservation of mass in integral form:

$$\frac{\partial}{\partial t}\int_V C dV = -\int_S C\bar{V}.\bar{n}dA + \int_S D_n \frac{\partial C}{\partial n} dA. \tag{2.63}$$

For any arbitrary volume the integral must be zero and the two surface integrals reduce to a sum fluxes across the six cube faces and we have:

$$\frac{\partial C}{\partial t} dV = \sum_{i=1}^{N} \left[-C\bar{V}.\bar{n}dA + D_n \frac{\partial C}{\partial n} dA \right], \tag{2.64}$$

and $\bar{V}.\bar{n} = -u$ and $\frac{\partial C}{\partial n} = -\frac{\partial C}{\partial x}$. The net flux in $X = \left[-\frac{\partial uC}{\partial x} + \frac{\partial}{\partial x} D_x \frac{\partial C}{\partial x} \right] \partial x \partial y \partial z$, where $dV = \partial x \partial y \partial z$. The differential form of conservation of mass is:

$$\frac{\partial C}{\partial t} = -\frac{\partial uC}{\partial x} - \frac{\partial vC}{\partial y} - \frac{\partial wC}{\partial z} + \frac{\partial}{\partial x} D_x \frac{\partial C}{\partial x} + \frac{\partial}{\partial y} D_y \frac{\partial C}{\partial y} + \frac{\partial}{\partial z} D_z \frac{\partial C}{\partial z}. \tag{2.65}$$

Simplifying this expression, considering the advective fluxes in equation (2.65), we have,

$$\frac{\partial uC}{\partial x} + \frac{\partial vC}{\partial y} + \frac{\partial wC}{\partial z} = \left[\frac{\partial u}{\partial x} + \frac{\partial v}{\partial y} + \frac{\partial w}{\partial z} \right] C + u \frac{\partial C}{\partial x} + v \frac{\partial C}{\partial y} + w \frac{\partial C}{\partial z}. \tag{2.66}$$

For incompressible flow, we know that: $\frac{\partial u}{\partial x} + \frac{\partial v}{\partial y} + \frac{\partial w}{\partial z} = 0$ from continuity equation and also considering the $y-$ direction and function of t we have the conservation of mass as:

$$\frac{\partial C}{\partial t} + v\frac{\partial C}{\partial y} = D_m \frac{\partial^2 C}{\partial y^2}. \tag{2.67}$$

For this work, we add the term for diffusion on temperature and the thermal conductivity of concentration of the fluid, therefore the mass conservation equation is:

$$\frac{\partial C}{\partial t} + v\frac{\partial C}{\partial y} = D_m \frac{\partial^2 C}{\partial y^2} + \frac{D_m k_T}{T_m}\frac{\partial^2 T}{\partial y^2} - k_c(C - C_\infty). \tag{2.68}$$

2.1.5 Analysis of the problem

We now study an unsteady two-dimensional MHD mixed convection flow of an incompressible and electrically conducting viscous fluid passing along an infinite vertical plate with Dufour and Soret effects. Following Vedavathi et.al [45], the x-axis is taken on the infinite plate, and parallel to the free-stream velocity which is vertical and the y-axis is taken as normal to the plate. A uniform magnetic field B_0 is applied in the y-direction of the flow. Initially the plate and the fluid are at the same temperature T_∞ in a stationary condition with concentration level C_∞ at all points. For $t > 0$, the plate starts moving impulsively with a velocity u_0 and its temperature is raised to T_w and the concentration level of the plate is raised to C_w. In this study we are numerically analysing the unsteady MHD mixed convection flow using the continuity, momentum, energy and mass diffusion equations referring to Vedavathi et.al [45], together with the addae terms, we have the following system of PDEs:

$$\begin{aligned}
\frac{\partial v}{\partial y} &= 0, && (2.69)\\
\frac{\partial u}{\partial t} + v\frac{\partial u}{\partial y} &= \nu\frac{\partial^2 u}{\partial y^2} + g\beta_t(T - T_\infty) + \\
&\quad g\beta_c(C - C_\infty) - \frac{\sigma B_0^2}{\rho}u - \frac{\nu}{K}u - \frac{b}{K}u^2, && (2.70)\\
\frac{\partial T}{\partial t} + v\frac{\partial T}{\partial y} &= \alpha\frac{\partial^2 T}{\partial y^2} - \frac{1}{\rho c_p}\frac{\partial q_r}{\partial y} + \frac{D_m k_T}{c_s c_p}\frac{\partial^2 C}{\partial y^2} + \frac{\mu}{\rho c_p}\left(\frac{\partial u}{\partial y}\right)^2, && (2.71)\\
\frac{\partial C}{\partial t} + v\frac{\partial C}{\partial y} &= D_m\frac{\partial^2 C}{\partial y^2} + \frac{D_m k_T}{T_m}\frac{\partial^2 T}{\partial y^2} - k_c(C - C_\infty), && (2.72)
\end{aligned}$$

with boundary conditions:

$$u = u_0, \quad v = v(t), \quad T = T_w, \quad C = C_w \quad at \quad y = 0, \tag{2.73}$$

$$u = 0, \quad v = 0, \quad T = T_\infty, \quad C = C_\infty \quad at \quad y \to \infty. \tag{2.74}$$

Where u, v are velocity components along $x-$axis and $y-$axis respectively, t is the time, υ is the kinematic viscosity, g is the acceleration due to gravity, T and T_∞ are the fluid temperature within the boundary layer and in the free-stream respectively, C and C_∞ is the concentration of the fluid within the boundary layer and far from the sheet respectively, C_w is the wall concentration, σ is the electric conductivity, B_0 is the uniform magnetic field strength (magnetic induction), ρ is density of the fluid, c_p the specific heat at constant pressure, c_s is the concentration susceptibility, D_m is the diffusion coefficient, T_m is the mean fluid temperature, k_T is the thermal diffusion ratio, K is the Darcy permeability, b is the empirical constant, T is the thermal temperature inside the thermal boundary layer and C is the corresponding concentration, α is the thermal diffusivity, k_c is the thermal conductivity of the concentration of the fluid, q_r is the component of radiative heat flux, β_t and β_c are the thermal and concentration expansion coefficients respectively. From (2.66), υ is either a constant or a function of time. Following Mohammed Ibrahim et al.[14], we have

$$v = v(t) = -c\left(\frac{\nu}{t}\right)^{\frac{1}{2}}, \tag{2.75}$$

where $c > 0$ is the suction parameter.

2.2 Similarity Technique

In this section the overview of similarity technique will be covered and the boundary-layer equations will be transformed into ordinary differential equations.

2.2.1 Similarity Transformation

The problem formulation results to a system of partial differential equations that are not easy to solve, hence the similarity transformations are used to reduce the partial

differential equations into ordinary differential equations. These ordinary differential equations are coupled and can be solved by numerical methods.

In this study, we introduce the similarity variables from Mohammed Ibrahim et al.[14] to convert the partial differential equations and their boundary conditions into ordinary differential equations, i.e,

$$\eta = \frac{y}{2\sqrt{\nu t}}, \quad y = \frac{2\nu^{1/2}\eta}{t^{-1/2}}, \quad u = u_0 f(\eta), \quad \theta = \frac{T - T_\infty}{T_w - T_\infty}, \ \phi = \frac{C - C_\infty}{C_w - C_\infty}, \tag{2.76}$$

we have,

$$v = \frac{-c\nu^{\frac{1}{2}}}{t^{\frac{1}{2}}}, \quad \frac{\partial \eta}{\partial y} = \frac{1}{2\nu^{\frac{1}{2}} t^{\frac{1}{2}}}, \quad \frac{\partial \eta}{\partial t} = \frac{-\eta}{2t}. \tag{2.77}$$

2.2.2 Similarity Transformation for Continuity Equation

$$\frac{\partial v}{\partial y} = \frac{\partial}{\partial y}(-c(\nu^{1/2}t^{-1/2})) \times \frac{\partial \eta}{\partial y} = -c\nu f' = 0.$$

dividing by $-c\nu$ we have: $f' = 0$.

2.2.3 Similarity Transformation for Momentum Equation

$$\frac{\partial u}{\partial t} + v\frac{\partial u}{\partial y} = \nu\frac{\partial^2 u}{\partial y^2} + g\beta_t(T - T_\infty) + g\beta_c(C - C_\infty) - \frac{\sigma B_0^2}{\rho}u - \frac{\nu}{K}u - \frac{b}{K}u^2.$$

$$\frac{\partial u}{\partial t} = \frac{\partial (Uf(\eta))}{\partial \eta} \times \frac{\partial \eta}{\partial t} = Uf' \times \frac{-\eta}{2t} = -\frac{U\eta f'}{2t}.$$

$$\frac{\partial u}{\partial y} = \frac{\partial (Uf(\eta))}{\partial \eta} \times \frac{\partial \eta}{\partial y} = Uf' \times \frac{1}{2\sqrt{\nu t}} = \frac{Uf'}{2\nu^{1/2}t^{1/2}},$$

therefore,

$$v\frac{\partial u}{\partial y} = \frac{-c\nu^{1/2}}{t^{1/2}} \times \frac{Uf'}{2\nu^{1/2}t^{1/2}} = \frac{-cUf'}{2t},$$

and

$$\nu\frac{\partial^2 u}{\partial y^2} = \nu\frac{\partial}{\partial y}\left(\frac{\partial u}{\partial y}\right) = \nu\frac{\partial}{\partial \eta}\left(\frac{Uf'}{2\nu^{1/2}t^{1/2}}\right) \times \frac{\partial \eta}{\partial y} = \nu\frac{Uf''}{2\nu^{\frac{1}{2}}t^{\frac{1}{2}}} \times \frac{1}{2\nu^{\frac{1}{2}}t^{\frac{1}{2}}} = \frac{Uf''}{4t}.$$

$$g\beta_t(T - T_\infty) = g\beta_t(T_\infty + \theta(T_w - T_\infty) - T_\infty) = g\beta_t\theta(T_w - T_\infty) = \theta g\beta_t(T_w - T_\infty).$$

$$g\beta_c(C - C_\infty) = g\beta_c(C_\infty + \phi(C_w - C_\infty) - C_\infty) = g\beta_c\phi(C_w - C_\infty) = \phi g\beta_c(C_w - C_\infty).$$

$$-\frac{\sigma B_0^2}{\rho}u = -\frac{\sigma B_0^2}{\rho}Uf, \quad -\frac{\nu}{K}u = -\frac{\nu}{K}Uf, \quad -\frac{b}{K}u^2 = -\frac{b}{K}U^2f^2.$$

Substituting above expressions into the momentum equation we have:

$$-\frac{Uf'\eta}{2t} - \frac{cUf'}{2t} = \frac{Uf''}{4t} + \theta g\beta_t(T_w - T_\infty) + \phi g\beta_c(C_w - C_\infty) - \frac{\sigma B_0^2}{\rho}Uf - \frac{\nu}{K}Uf - \frac{b}{K}U^2f^2,$$

multiplying by $\frac{2t}{U}$, we get:

$$-\eta f' - cf' = \frac{f''}{2} + \frac{g\beta_t 2t}{U}(T_w - T_\infty)\theta + \frac{g\beta_c 2t}{U}(C_w - C_\infty)\phi - \frac{2t\sigma B_0^2}{\rho}f - \frac{2t\nu}{K}f - \frac{2tb}{K}f^2,$$

multiplying by 2, we have:

$$f'' + 2(\eta + c)f' + \frac{g\beta_t 4t}{U}(T_w - T_\infty)\theta + \frac{g\beta_c 4t}{U}(C_w - C_\infty)\phi - \frac{4t\sigma B_0^2}{\rho}f - \frac{4t\nu}{K}f - \frac{4tb}{K}f^2 = 0,$$

hence the transformed momentum equation is given by:

$$f'' + 2(\eta + c)f' + Gr\theta + Gc\phi - Mf - \frac{1}{Da}f - \frac{ReFs}{Da}f^2 = 0.$$

2.2.4 Similarity Transformation for Energy Equation

$$\frac{\partial T}{\partial t}+v\frac{\partial T}{\partial y}=\alpha\frac{\partial^2 T}{\partial y^2}-\frac{1}{\rho c_p}\frac{\partial q_r}{\partial y}+\frac{D_m k_T}{c_s c_p}\frac{\partial^2 C}{\partial y^2}+\frac{\mu}{\rho c_p}\left(\frac{\partial u}{\partial y}\right)^2.$$

$$\frac{\partial T}{\partial t}=\frac{\partial(T_\infty+\theta(T_w-T_\infty))}{\partial t}=(T_w-T_\infty)\frac{\partial\theta}{\partial\eta}\times\frac{\partial\eta}{\partial t}=-\frac{(T_w-T_\infty)\theta'\eta}{2t}.$$

$$\frac{\partial T}{\partial y}=\frac{\partial(T_\infty+\theta(T_w-T_\infty))}{\partial y}=(T_w-T_\infty)\frac{\partial\theta}{\partial\eta}\times\frac{\partial\eta}{\partial y}=\frac{(T_w-T_\infty)\theta'}{2\nu^{1/2}t^{1/2}},$$

therefore,

$$v\frac{\partial T}{\partial y}=-c\frac{\nu^{1/2}}{t^{1/2}}\times\frac{(T_w-T_\infty)\theta'}{2\nu^{1/2}t^{1/2}}=\frac{-c(T_w-T_\infty)\theta'}{2t},$$

and

$$\frac{\partial^2 T}{\partial y^2}=\frac{\partial(\frac{(T_w-T_\infty)\theta'}{2\nu^{1/2}t^{1/2}})}{\partial y}=\frac{(T_w-T_\infty)}{2\nu^{1/2}t1/2}\times\frac{\partial\theta'}{\partial\eta}\times\frac{\partial\eta}{\partial y}=\frac{(T_w-T_\infty)\theta''}{2\nu^{1/2}t^{1/2}}\times\frac{1}{2\nu^{1/2}t^{1/2}}=\frac{(T_w-T_\infty)\theta''}{4\nu t},$$

therefore,

$$\alpha\frac{\partial^2 T}{\partial y^2}=\frac{\alpha(T_w-T_\infty)\theta''}{4\nu t}.$$

$$\frac{\partial q_r}{\partial y},\qquad q_r=-\frac{4\sigma_s}{3k_e}\frac{\partial T^4}{\partial y},\qquad T^4=4T_\infty^3T-3T_\infty^4,$$

$$\frac{\partial T^4}{\partial y}=\frac{\partial(4T_\infty^3T-3T_\infty^4)}{\partial y}=4T_\infty^3\frac{\partial T}{\partial y},$$

therefore,

$$q_r=-\frac{4\sigma_s}{3k_e}4T_\infty^3\frac{\partial T}{\partial y}=-\frac{16\sigma_sT_\infty^3}{3k_e}\frac{\partial T}{\partial y},$$

$$\frac{\partial q_r}{\partial y}=\frac{\partial(-\frac{16\sigma_sT_\infty^3}{3k_e}\frac{\partial T}{\partial y})}{\partial y}=-\frac{16\sigma_sT_\infty^3}{3k_e}\frac{\partial^2 T}{\partial y^2},$$

then,

$$\frac{1}{\rho c_p}\frac{\partial q_r}{\partial y} = -\frac{16\sigma_s T_\infty^3}{3\rho c_p k_e}\frac{\partial^2 T}{\partial y^2} = -\frac{16\sigma_s T_\infty^3 (T_w - T_\infty)}{12\rho c_p k_e \nu t}\theta''.$$

$$\frac{\partial^2 C}{\partial y^2} = \frac{\partial(\frac{(C_w - C_\infty)\phi}{2\nu^{1/2}t^{1/2}})}{\partial y} = \frac{(C_w - C_\infty)}{2\nu^{1/2}t^{1/2}}\frac{\partial \phi'}{\partial \eta}\frac{\partial \eta}{\partial y} = \frac{(C_w - C_\infty)}{2\nu^{1/2}t^{1/2}}\phi''\frac{1}{2\nu^{1/2}t^{1/2}} = \frac{(C_w - C_\infty)}{4\nu t}\phi'',$$

therefore,

$$\frac{D_m K_T}{c_s c_p}\frac{\partial^2 C}{\partial y^2} = \frac{D_m K_T}{c_s c_p}\frac{(C_w - C_\infty)}{4\nu t}\phi''.$$

$$\frac{\partial u}{\partial y} = \frac{\partial (Uf)}{\partial \eta}\frac{\partial \eta}{\partial y} = \frac{Uf'}{2\nu^{1/2}t^{1/2}},$$

therefore,

$$\frac{\mu}{\rho c_p}\left(\frac{\partial u}{\partial y}\right)^2 = \frac{\mu}{\rho c_p}\frac{U^2 f'^2}{4\nu t}.$$

We substitute above expressions into the energy equation, to get:

$$\frac{(T_w - T_\infty)\theta'\eta}{2t} + \frac{c(T_w - T_\infty)\theta'}{2t} + \frac{\alpha(T_w - T_\infty)\theta''}{4\nu t} + \frac{16\sigma_s T_\infty^3 (T_w - T_\infty)}{12\rho c_p k_e \nu t}\theta'' + \frac{D_m K_T}{c_s c_p}\frac{(C_w - C_\infty)}{4\nu t}\phi'' + \frac{\mu}{\rho c_p}\frac{U^2 f'^2}{4\nu t} = 0,$$

dividing above expression by $\frac{(T_w - T_\infty)}{4t}$ we get:

$$\frac{\alpha}{\nu}\theta'' + \frac{16\sigma_s T_\infty^3}{3\rho\nu c_p k_e}\theta'' + 2\eta\theta' + 2c\theta' + \frac{D_m K_T}{c_s c_p \nu}\frac{(C_w - C_\infty)}{T_w - T_\infty}\phi'' + \frac{\mu U^2}{\rho\nu c_p (T_w - T_\infty)}f'^2 = 0,$$

$$\left(\frac{\alpha}{\nu} + \frac{16\sigma_s T_\infty^3}{3\rho\nu c_p k_e}\right)\theta'' + 2(\eta + c)\theta' + \frac{D_m K_T}{c_s c_p \nu}\frac{(C_w - C_\infty)}{T_w - T_\infty}\phi'' + \frac{\mu U^2}{\rho\nu c_p (T_w - T_\infty)}f'^2 = 0,$$

then finally the energy equation is given by:

$$\left(\frac{1}{Pr} + R\right)\theta'' + 2(\eta + c)\theta' + Du\phi'' + Ecf'^2 = 0.$$

2.2.5 Similarity Transformation for Mass Diffusion Equation

$$\frac{\partial C}{\partial t} + v\frac{\partial C}{\partial y} = D_m\frac{\partial^2 C}{\partial y^2} + \frac{D_m k_T}{T_m}\frac{\partial^2 T}{\partial y^2} - k_c(C - C\infty).$$

$$\frac{\partial C}{\partial t} = \frac{\partial(C_\infty + \phi(C_w - C_\infty))}{\partial t} = (C_w - C_\infty)\frac{\partial \phi}{\partial \eta}\frac{\partial \eta}{\partial t} = -\frac{(C_w - C_\infty)\eta}{2t}\phi'.$$

$$\frac{\partial C}{\partial y} = (C_w - C_\infty)\frac{\partial \phi}{\partial \eta}\frac{\partial \eta}{\partial y} = \frac{(C_w - C_\infty)}{2\nu^{1/2}t^{1/2}}\phi',$$

therefore,

$$v\frac{\partial C}{\partial y} = -c\frac{\nu^{1/2}}{t^{1/2}}\frac{(C_w - C_\infty)}{2\nu^{1/2}t^{1/2}}\phi' = -\frac{c(C_w - C_\infty)}{2t}\phi',$$

$$\frac{\partial^2 C}{\partial y^2} = \frac{\partial \frac{(\phi'(C_w - C_\infty))\phi'}{2\nu^{1/2}t^{1/2}}}{\partial \eta}\frac{\partial \eta}{\partial y} = \frac{(C_w - C_\infty)}{2\nu^{1/2}t^{1/2}}\phi''\frac{1}{2\nu^{1/2}t^{1/2}} = \frac{(C_w - C_\infty)}{4\nu t}\phi'',$$

and

$$D_m\frac{\partial^2 C}{\partial y^2} = \frac{D_m(C_w - C_\infty)}{4\nu t}\phi''.$$

$$\frac{\partial^2 T}{\partial y^2} = \frac{\partial \frac{(\theta'(T_w - T_\infty))}{2\nu^{1/2}t^{1/2}}}{\partial \eta}\frac{\partial \eta}{\partial y} = (T_w - T_\infty)\frac{\theta''}{2\nu^{1/2}t^{1/2}}\frac{1}{2\nu^{1/2}t^{1/2}} = \frac{(T_w - T_\infty)}{4\nu t}\theta'',$$

$$\frac{D_m K_T}{T_m}\frac{\partial^2 T}{\partial y^2} = \frac{D_m K_T(T_w - T_\infty)}{4T_m\nu t}\theta''.$$

$$-k_c(C - C_\infty) = -k_c(C_\infty + \phi(C_w - C_\infty) - C_\infty) = -k_c\phi(C_w - C_\infty).$$

We substitute the above equations into the concentration equation, to get:

$$-\frac{(C_w - C_\infty)\eta}{2t}\phi' - \frac{c(C_w - C_\infty)}{2t}\phi' = \frac{D_m(C_w - C_\infty)}{4\nu t}\phi'' + \frac{D_m K_T(T_w - T_\infty)}{4T_m\nu t}\theta'' - k_c\phi(C_w - C_\infty),$$

dividing above expression by $\frac{C_w - C_\infty}{4t}$ we get:

$$-2\eta\phi' - 2c\phi' = \frac{D_m}{\nu}\phi'' + \frac{D_m K_T(T_w - T_\infty)}{T_m \nu(C_w - C_\infty)}\theta'' - 4k_c t\phi,$$

$$\frac{D_m}{\nu}\phi'' + 2(\eta + c)\phi' + \frac{D_m K_T(T_w - T_\infty)}{T_m \nu(C_w - C_\infty)}\theta'' - 4k_c t\phi = 0,$$

hence the concentration equation is given by:

$$\frac{1}{Sc}\phi'' + 2(\eta + c)\phi' + Sr\theta'' - Kr\phi = 0.$$

2.2.6 Similarity Transformation for Boundary Conditions

$$u = u_0, \quad v = v(t), \quad T = T_w, \quad C = C_w \quad \text{at} \quad y = 0,$$

$$u = 0, \quad T = T_\infty, \quad C = C_\infty, \quad as \quad y \longrightarrow \infty.$$

at $\eta = 0$, we have:

$$u = u_0 f(\eta),$$

$$u(0) = u_0 f(0),$$

$$f(0) = 1.$$

The v boundary will vanish since v is constant.

$$T = T_w,$$

$$T_\infty + \theta(T_w - T_\infty) = T_w,$$

$$\theta(T_w - T_\infty) = T_w - T_\infty,$$

$$\theta = \frac{T_w - T_\infty}{T_w - T_\infty},$$

$$\theta = 1.$$

$$C = C_w,$$

$$C_\infty + \phi(C_w - C_\infty) = C_w,$$

$$\phi(C_w - C_\infty) = C_w - C_\infty,$$

$$\phi = \frac{C_w - C_\infty}{C_w - C_\infty},$$

$$\phi = 1,$$

at $\eta \to \infty$, we have:

$$u = u_0 f(\eta),$$

$$u(\infty) = u_0 f(\infty),$$

$$f(\infty) \to \infty.$$

$$T = T_\infty,$$

$$T_\infty + \theta(T_w - T_\infty) = T_\infty,$$

$$\theta(T_w - T_\infty) = T_\infty - T_\infty,$$

$$\theta = \frac{T_\infty - T_\infty}{T_w - T_\infty},$$

$$\theta \to 0.$$

$$C = C_\infty,$$

$$C_\infty + \phi(C_w - C_\infty) = C_\infty,$$

$$\phi(C_w - C_\infty) = C_\infty - C_\infty,$$

$$\phi = \frac{C_\infty - C_\infty}{C_w - C_\infty},$$

$$\phi \to 0.$$

Transformed ordinary differential equations and their boundary conditions are then given as:

$$f' = 0, \tag{2.78}$$

$$f'' + 2(\eta + c)f' + Gr\theta + Gc\phi - Mf - \frac{1}{Da}f - \frac{ReFs}{Da}f^2 = 0, \tag{2.79}$$

$$\left(\frac{1}{Pr} + R\right)\theta'' + 2(\eta + c)\theta' + Du\phi'' + Ecf'^2 = 0, \tag{2.80}$$

$$\frac{1}{Sc}\phi'' + 2(\eta + c)\phi' + Sr\theta'' - Kr\phi = 0, \tag{2.81}$$

with boundary conditions:

$$f(0) = 1, \quad \theta = 1, \quad \phi = 1 \quad \text{at} \quad \eta = 0, \tag{2.82}$$

$$f \to 0, \quad \theta \to 0, \quad \phi \to \quad as \quad \eta \to \infty. \tag{2.83}$$

Chapter 3

Methodology

In this chapter, we conduct a literature review on the Spectral Local Linearization Method (SLLM) and implementation of the SLLM for the present nonlinear coupled system of differential equations and test its convergence.

3.1 The SLLM

The Spectral Local Linearization method was developed by Motsa [26], for non-linear boundary value problems that arise in similarity variable boundary layer flow applications. The SLLM is based on, decoupling and linearizing systems of equations using a combination of a univariate linearization technique and a spectral collocation discretization. The key feature of the SLLM algorithm is that it breaks down a large coupled system of equations into a sequence of smaller subsystems which can be solved sequentially in a very computationally efficient manner.

Spectral methods are becoming the preferred tools for solving ordinary and partial differential equations because of their elegance and high accuracy in resolving problems with smooth functions. Motsa [26], has outlined the observations made about the proposed SLLM. He noticed that the algorithm of the SLLM is very easy to develop and implement, as it is based on a simple univariate linearization of nonlinear functions. The method is numerically efficient, since it results in a series of equations which are solved in a sequential manner by reusing the information from the solution of one equation in

the next equation. The method was found to converge rapidly to the expected solutions for all the input parameters considered in their study.

Motsa et al. [27], introduced the Spectral Local Linearization approach for natural convection boundary layer flow. The SLLM results were found to be consistent with results available in the literature. Mixed Convection and Nonlinear Radiation in the Stagnation Point Nanofluid flow towards a Stretching Sheet with Homogenous-Heterogeneous Reactions effects was explored by Das et al. [9]. The SLLM was used as the method solution. It is observed that the accuracy of the method used was quite excellent in agrement with the previous data available in the literature in their study.

Shateyi and Marewo [38], employed a new numerical analysis of the hall effect on MHD flow and heat transfer over an unsteady stretching permeable surface in the presence of thermal radiation and heat source/sink. Employing a computational iteration approach known as the Spectral Local Linearization method and they compared the results with those obtained using the Matlab `bvp4c` technique. Much attention was given to investigating how the velocity field, skin-friction, temperature distribution and heat transfer are influenced by the important parameters. The investigations showed an agreement between the results obtained using SLLM and those obtained using `bvp4c`.

3.1.1 Description of the SLLM

Consider a system of m non-linear ordinary differential equations in m unknown functions $Z_i(\eta)$ i=1,2,...,m where $\eta \in [a, b]$ is the independent variable. The system can be written in terms of Z_i as a sum of it's linear (L_i) and non-linear components (N_i) as:

$$L_i[Z_1, Z_2, ..., Z_m] + N_i[Z_1, Z_2, ..., Z_m] = H_i, \quad i = 1, ..., m, \tag{3.1}$$

where $H(\eta)$ is a known function of η. To develop the iteration scheme, we apply local linearisation of N_i about $Z_{i,r}$ (the previous iteration) to the ith non-linear equation assuming that all other $Z_k, r(k \neq i)$ are known. Thus, at the ith equation, N_i is linearised as follows:

$$N_i[Z_1, Z_2, ..., m] = N_i[Z_{1,r}, Z_{2,r}, ..., Z_m] + \frac{\partial N_i}{\partial Z_i}[Z_{1,r}, Z_{2,r}, ..., Z_m](Z_i - Z_{i,r}), \tag{3.2}$$

$$L_i[Z_{1,r+1}, ..., Z_m] + \frac{\partial N_i}{\partial Z_i}[...]Z_{i,r+1} = H_i + \frac{\partial N_i}{\partial Z_i}[...]Z_{i,r} - N_i[Z_{1,r}, ..., Z_{m,r}]. \tag{3.3}$$

where [...]denotes $[Z_{1,r}, Z_{2,r}, ..., Z_m]$ and $Z_{i,r+1}$ and $Z_{i,r}$ are the approximations of Z at the current and previous iteration, respectively. Thus, starting from an initial approximation $Z_{1,0}, Z_{2,0}, ..., Z_{m,0}$. The proposed iteration scheme (3.3), is then solved iteratively until the system converges at a consistent solution for all variables. To solve the iteration scheme (3.3), it is convenient to use the Chebyshev pseudo-spectral method. For this reason, the proposed method is referred to as the Spectral Local Linearization iteration method (SLLM) in this work. Before applying the spectral method, it is convenient to transform the domain on which the governing equation is defined to the interval [-1,1] on which the spectral method can be implemented. The transformation $\eta = (b-a)(\tau+1)/2$ is used to map the interval $[a, b]$ to $[-1, 1]$. The basic idea behind the spectral collocation method is the introduction of a differentiation matrix D which is used to approximate the derivatives of the unknown variables $Z_i(\eta)$ at the collocation points as the matrix vector product.

$$\frac{dZ_i}{d\eta} = \sum_{k=0}^{\bar{N}} \mathbf{D}_{lk} Z_i(\tau_k) = \mathbf{D}\mathbf{Z}_i, \quad l = 0, 1, ..., \bar{N}, \tag{3.4}$$

where $\bar{N} + 1$ is the number of collocation points (grid points), $\mathbf{D} = 2D/(b-a)$, and $\mathbf{Z} = [z(\tau_0), z(\tau_1), ..., z(\tau_N)]^T$ is the vector function at the collocation points. Higher order derivatives are obtained as powers of $\mathbf{D}$, that is ${Z_j}^{(p)} = \mathbf{D}^p\mathbf{Z}_j$, where p is the order of the derivative.

3.1.2 Application of SLLM

This section outlines the application of the SLLM in solving the transformed equations. The following equations from chapter 2 are solved as follows:

$$f' = 0, \tag{3.5}$$

$$f'' + 2(\eta + c)f' + Gr\theta + Gc\phi - Mf - \frac{1}{Da}f - \frac{ReFs}{Da}f^2 = 0, \tag{3.6}$$

$$\left(\frac{1}{Pr} + R\right)\theta'' + 2(\eta + c)\theta' + Du\phi'' + Ecf'^2 = 0, \tag{3.7}$$

$$\frac{1}{Sc}\phi'' + 2(\eta + c)\phi' + Sr\theta'' - Kr\phi = 0. \tag{3.8}$$

Equations (3.5) - (3.8) may be written as:

$$L_1 + N_1 = H_1, \tag{3.9}$$

$$L_2 + N_2 = H_2, \tag{3.10}$$

$$L_3 + N_3 = H_3, \tag{3.11}$$

$$L_4 + N_4 = H_4, \tag{3.12}$$

where,

$$L_1 = f', \quad N_1 = 0, \quad H_1 = 0. \tag{3.13}$$

$$L_2 = f'' + 2(\eta + c)f' + Gr\theta + Gc\phi - Mf - \frac{1}{Da}f, \quad N_2 = -\frac{ReFs}{Da}f^2,$$

$$H_2 = 0. \tag{3.14}$$

$$L_3 = \left(\frac{1}{Pr} + R\right)\theta'' + 2(\eta + c)\theta' + Du\phi'', \quad N_3 = Ecf'^2, \quad H_3 = 0. \tag{3.15}$$

$$L_4 = \frac{1}{Sc}\phi'' + 2(\eta + c)\phi' + Sr\theta'' - Kr\phi, \quad N_4 = 0, \quad H_4 = 0. \tag{3.16}$$

Using equation (3.3), we obtain:

$$\begin{aligned} f''_{r+1} + 2(\eta + c)f'_{r+1} - (M + \frac{1}{Da})f_{r+1} - \frac{2ReFs}{Da}f_r f_{r+1} &= -\frac{ReFs}{Da}f_r^2 - Gr\theta_r \\ -Gc\phi_r, & \end{aligned} \tag{3.17}$$

$$\begin{aligned} \left(\frac{1}{Pr} + R - ScSrDu\right)\theta''_{r+1} + 2(\eta + c)\theta'_{r+1} &= -Ecf'^2_r + \\ 2(\eta + c)ScDu\phi'_r - KrScDu\phi_r, & \end{aligned} \tag{3.18}$$

$$\begin{aligned} \left(\frac{1}{Sr} + R - \frac{DuPrSr}{1 + PrR}\right)\phi''_{r+1} + 2(\eta + c)\phi'_{r+1} + Kr\phi_{r+1} &= \frac{2(\eta + c)PrSr}{1 + PrR}\theta'_r \\ + \frac{EcSrPr}{1 + PrR}f'^2_r, & \end{aligned} \tag{3.19}$$

subjected to boundary conditions:

$$f_{r+1}(0) = 1, \quad \theta_{r+1}(0) = 1, \quad \phi_{r+1}(0) = 1, \tag{3.20}$$

$$f_{r+1}(\infty) = 0, \quad \theta_{r+1}(\infty) = 0, \quad \phi_{r+1}(\infty) = 0. \tag{3.21}$$

Applying the Chebyshev pseudo-spectral method on equations (3.17) - (3.19) we obtain the following equation:

$$\mathbf{A}_1 = \left(\frac{1}{Sc} - \frac{DuPrSr}{1+Pr}\right)\mathbf{D}^2 + \mathbf{diag}\left\{2(\eta+c)\right\}\mathbf{D} - Kr\mathbf{I},$$

$$\mathbf{B}_1 = \frac{EcSrPr}{1+PrR} fr'^2 + \frac{2(\eta+c)PrSr}{1+PrR}\theta'_r, \tag{3.22}$$

$$\mathbf{A}_2 = \left(\frac{1}{Pr} + R - ScSrDu\right)\mathbf{D}^2 + \mathbf{diag}\left\{2(\eta+c)\right\}\mathbf{D},$$

$$\mathbf{B}_2 = -Ecfr'^2 + 2(\eta+c)ScDu\phi'_r - KrScDu\phi_r, \tag{3.23}$$

$$\mathbf{A}_3 = \mathbf{D}^2 + diag2(\eta+c)\mathbf{D} - \frac{2ReFs}{Da}\mathbf{diag}\left\{g_r\right\} - (M + \frac{1}{D_a})I$$

$$\mathbf{B}_3 = \frac{-ReFs}{Da} f_r^2 - Gr\theta_r - Gc\phi_r, \tag{3.24}$$

where I is the identity matrix of size $(N+1)\times(N+1)$ and $N+1$ is the grid points. Initial guesses satisfying the boundary conditions (2.78) and (2.79) are given as:

$$f_0(\eta) = 1 - e^{-\eta}, \tag{3.25}$$

$$\theta_0(\eta) = e^{-\eta}, \tag{3.26}$$

$$\phi_0(\eta) = e^{-\eta}, \tag{3.27}$$

The application of the SLLM generates approximations f_{r+1}, θ_{r+1}, ϕ_{r+1} for each $r = 0, 1, 2, ...$

3.2 Parameters of engineering interest

In this section we outline the engineering parameters of interest for the present study, which are the skin-friction coefficient, the Nusselt number and the sherwood number.

3.2.1 Skin-friction

The skin-friction at the plate can be obtained in non-dimensional form and is given by:

$$C_f = \frac{2\tau_w}{\rho U\sqrt{\nu t}} = \frac{2\mu}{\rho U\sqrt{\nu t}}\left(\frac{\partial u}{\partial y}\right)_{y=0} = (R_e)^{-1} f'(0). \tag{3.28}$$

where $\tau_w = \mu\left(\frac{\partial u}{\partial y}\right)_{y=0}$.

3.2.2 Nusselt number

The heat transfer rate in terms of the Nusselt number is given by:

$$N_u = \frac{2q_w\sqrt{\nu t}}{K(T_w - T_\infty)} = \frac{-2K\sqrt{\nu t}}{K(T_w - T_\infty)}\left(\frac{\partial T}{\partial y}\right)_{y=0} = -\theta'(0). \tag{3.29}$$

where $q_w = -K\left(\frac{\partial T}{\partial Y}\right)_{y=0}$.

3.2.3 Sherwood number

The mass transfer rate in the terms of Sherwood number is given by:

$$Sh = \frac{2M_w\sqrt{\nu t}}{D(C_w - C_\infty)} = \frac{-2D\sqrt{\nu t}}{D(C_w - C_\infty)}\left(\frac{\partial C}{\partial y}\right)_{y=0} = -\phi'(0). \tag{3.30}$$

where $M_w = -D\left(\frac{\partial C}{\partial Y}\right)_{y=0}$.

3.3 Test for convergence

The literature for testing for convergence is drawn from Madoda [20]. To analyse the convergence of the iterative scheme we consider the error due to decoupling (E_d) of the unknown functions for each $(r+1)^{th}$ iteration. E_d is basically the infinity norm of the solutions of each unknown between two successive iterations. That is:

$$E_d = max\left\{||Z_{1,r+1} - Z1, r||_\infty, ||Z_{2,r+1} - Z_{2,r}||_\infty, ...||Z_{m,r+1} - Z_{m,r}||_\infty\right\}. \tag{3.31}$$

where $Z_i, i = 1, 2, ..., m$ are the governing unknown functions. Suppose the error due to decoupling at each i^{th} iteration is given by $e_i, i = 1, 2, .., N$, where N is the total number of iterations. Then the iterative scheme is said to be convergent if,

$$e_1 < e_2 < e_3 < ... < e_N. \tag{3.32}$$

This is to say that the iterative scheme is convergent if E_d is inversely proportional to the number of iterations.

In this study the convergence tolerance is set to be $\varepsilon = 10^{-8}$, and the iterative procedure is stopped if the following conditions are satisfied:

$$max\left\{||g_{r+1} - g_r||_\infty, ||\theta_{r+1} - \theta_r||_\infty, ||\phi_{r+1} - \phi_r||_\infty\right\} < \varepsilon. \tag{3.33}$$

Chapter 4

Results and Discussion

The numerical analysis of unsteady MHD mixed convection flow past an infinite vertical plate in the with Dufour and Soret effects with viscous dissipation has been considered using the Spectral Local Linearisation method (SLLM).

In this chapter we outline the numerical results for the dimensionless velocity, temperature and concentration distributions graphically and the numerical values of the Skin-friction, the Nusselt number and the Sherwood number which are $f'(0)$, $-\theta'(0)$, and $-\phi'(0)$, respectively are presented in tabular form. The collocation points are set to be $N = 120$ in all cases and the tolerance level is $\epsilon = 10^{-8}$. The following default parametric values are adopted: $Gr = 10.0$, $Gc = 5.0$, $M = 1.0$, $Da = 1.0$, $Re = 10.0$, $Fs = 0.09$, $Pr = 0.71$, $R = 1.0$, $Du = 0.03$, $Sr = 2.0$, $c = 1.0$, $Kr = 3.0$, $Ec = 0.1$, $Sc = 0.22$. The results presented in this study were compared with those obtained using Matlab in-built `bvp4c` solver to check the accuracy and validate the proposed method.

4.1 Discussion of results

The performance of the proposed method was compared against the results obtained by Matlab `bvp4c` method in Table 4.1. For different values of the magnetic field strength (M), we observe that the SLLM is the best method compared to Matlab bvp4c. From the table it is clearly seen that the computational run times for the SLLM are far less than those of the bvp4c. The SLLM converges faster than the bvp4c with higher values

of the magnetic field strength (M). We therefore conclude that the SLLM is the best method for this present study. Hence, the rest of the results displayed in tabular and graphical forms were generated using the SLLM.

Table 4.1: Comparison of SLLM and bvp4c for the effect of (M) on $f'(0)$.

M	it	cpu time	SLLM	cpu time	`bvp4c`
1	8	0.64	2.98947118	157.92	2.98947118
3	8	0.57	1.82052989	267.06	1.82052989
5	8	0.58	0.91247112	209.24	0.91247112
7	8	0.61	0.17327144	234.79	0.17327144

Table 4.2 displays the effect of the magnetic field strength (M) on the $f'(0)$, $-\theta'(0)$ and $-\phi'(0)$. From this table we observe that Skin-friction $f'(0)$ decreases with an increase in the magnetic field parameter (M). We can also observe that the Nusselt number $-\theta'(0)$ increases as the magnetic flied strength (M) increases. This is because the Lorentz force generated a friction on the flow which causes more heat energy, thus, the temperature of the fluid increases. The Sherwood number $-\phi'(0)$ also decreases with an increase in the magnetic field parameter (M).

Table 4.2: Effect of the magnetic field strength (M) on the $f'(0)$, $-\theta'(0)$ and $-\phi'(0)$.

M	time(sec)	$f'(0)$	$-\theta'(0)$	$-\phi'(0)$
0	0.62	3.72078848	1.24384723	0.59630160
1	0.66	2.98947118	1.26629643	0.58681482
2	0.55	2.36421196	1.28093752	0.58064642
3	0.61	1.82052982	1.29044856	0.57665776

Table 4.3 shows the influence of the Prandtl number (Pr) on the $f'(0)$, $-\theta'(0)$ and $-\phi'(0)$. Numerical results show that the increase of the Prandtl number (Pr) results in decreasing the Skin-friction coefficient $f'(0)$ and the Sherwood number $-\phi'(0)$, whereas the Nusselt number $-\theta'(0)$ increases. This is because when the Prandtl number (Pr) increases, the

thermal boundary layer thickness decreases and it causes the temperature to increase since the heat reaches the free-stream temperature quickly.

Table 4.3: Influence of the Prandtl number (Pr) on the $f'(0)$, $-\theta'(0)$ and $-\phi'(0)$.

Pr	time(sec)	$f'(0)$	$-\theta'(0)$	$-\phi'(0)$
0.5	0.62	3.26591971	1.07214698	0.66456452
1.0	0.59	2.75825607	1.46250338	0.50679237
1.5	0.55	2.53565768	1.68937516	0.41295283

In Table 4.4, we display the effects of the Eckert number (Ec) on the $f'(0)$, $-\theta'(0)$ and $-\phi'(0)$. The Nusselt number $-\theta'(0)$ is reduced as the value of the Eckert number (Ec) increases, while the Skin-friction and the Sherwood number increase. An increase in the Eckert number (Ec), yields a decrease in the rate of heat transfer. Therefore, by changing the Eckert number (Ec) wall temperature can be manipulated.

Table 4.4: Effects of the Eckert number (Ec) on the $f'(0)$, $-\theta'(0)$ and $-\phi'(0)$.

Ec	time(sec)	$f'(0)$	$-\theta'(0)$	$-\phi'(0)$
0	0.59	2.93378439	1.32170941	0.56396443
0.2	0.61	3.04716630	1.20778601	0.61096807
0.5	0.62	3.23429173	1.01016043	0.69272846

Table 4.5 shows the influence of the chemical reaction parameter (Kr) on the $f'(0)$, $-\theta'(0)$ and $-\phi'(0)$. It is observed that as the chemical reaction parameter (Kr) increases the Skin-friction $f'(0)$ decreases and the Sherwood number $-\phi'(0)$ increases, whereas the temperature of the fluid is not significant.

Table 4.6 presents the effects of the thermal Grashof number (Gr) on the $f'(0)$, $-\theta'(0)$ and $-\phi'(0)$. It can clearly be seen that the Skin-friction coefficient $f'(0)$ and the Sherwood number $-\phi'(0)$ decrease as the thermal Grashof number (Gr) decrease, whereas the Nusselt number $-\theta'(0)$ increase as Gr decrease.

Table 4.5: Influence of the chemical reaction parameter (Kr) on the $f'(0)$, $-\theta'(0)$ and $-\phi'(0)$.

Kr	time(sec)	$f'(0)$	$-\theta'(0)$	$-\phi'(0)$
0.5	0.63	3.07209961	1.26534543	0.50083271
1.5	0.62	2.91064144	1.26703551	0.66613823
2.0	0.59	2.85014609	1.26761220	0.73993428

Table 4.6: Effects of the thermal Grashof number (Gr) on the $f'(0)$, $-\theta'(0)$ and $-\phi'(0)$.

Gr	time(sec)	$f'(0)$	$-\theta'(0)$	$-\phi'(0)$
10.0	0.62	2.98947118	1.26629643	0.58681482
7.0	0.62	1.9249735	1.28822268	0.57756635
5.0	0.63	1.21357263	1.29792258	0.57351570

Table 4.7 presents the effects of the the modified Grashof number (Gc) on the $f'(0)$, $-\theta'(0)$ and $-\phi'(0)$. It can clearly be seen that the modified Grashof number (Gc) has the same effects on the Skin-friction coefficient $f(0)$, the Nusselt number $-\theta(0)$ and the Sherwood number $-\phi'(0)$ as the thermal Grashof number (Gr).

Table 4.7: Effects of the modified Grashof number (Gc) on the $f'(0)$, $-\theta'(0)$ and $-\phi'(0)$.

Gc	time(sec)	$f'(0)$	$-\theta'(0)$	$-\phi'(0)$
5.0	0.62	2.98947118	1.26629643	0.58681482
3.0	0.62	1.99524305	1.28594332	0.57852519
2.0	0.63	1.49055451	1.29237956	0.57583431

Numerical values of the Skin-friction $f'(0)$, Nusselt number $-\theta'(0)$ and the Sherwood number $-\phi'(0)$ are displayed in Table 4.8 for different values the Dufour number (Du). It can be clearly observed that as the Dufour number (Du) increases the Skin-friction $f'(0)$ and the Sherwood number $-\phi'(0)$ increases. Hence the Nusselt number decrease with an increase in Du.

Table 4.8: Effects of the Dufour number (Du) on the $f'(0)$, $-\theta'(0)$ and $-\phi'(0)$.

Du	time(sec)	$f'(0)$	$-\theta'(0)$	$-\phi'(0)$
0.03	0.66	2.98947118	1.26629643	0.58681482
0.05	0.63	2.99582553	1.26345968	0.58788761
0.07	0.64	3.00218730	1.26060507	0.58896797

Numerical values of the Skin-friction $f'(0)$, Nusselt number $-\theta'(0)$ and the Sherwood number $-\phi'(0)$ are displayed in Table 4.9 for different values the Soret number (Sr). It can be clearly observed that as the Soret number (Sr) decreases the Skin-friction $f'(0)$ and the Sherwood number $-\phi'(0)$ increase whereas the Nusselt number $-\theta'(0)$ increases.

Table 4.9: Effects of the Soret number (Sr) on the $f'(0)$, $-\theta'(0)$ and $-\phi'(0)$.

Sr	time(sec)	$f'(0)$	$-\theta'(0)$	$-\phi'(0)$
2.0	0.66	2.98947118	1.26629643	0.58681482
1.2	0.63	2.83811469	1.26786763	0.74437503
0.8	0.64	2.76197621	1.26851730	0.82337959

In Table 4.10 we display the influence of the suction parameter (c) on the $f'(0)$, $-\theta'(0)$ and $-\phi'(0)$. It is observed that an increase in the suction parameter (c), results in a decrease in the Skin-friction $f'(0)$ and an increase in the Nusselt number $-\theta'(0)$ and the Sherwood number $-\phi'(0)$.

Table 4.10: Influence of the suction parameter (c) on the $f'(0)$, $-\theta'(0)$ and $-\phi'(0)$.

c	time(sec)	$f'(0)$	$-\theta'(0)$	$-\phi'(0)$
0.25	0.60	3.64932947	0.77482612	0.58285805
0.50	0.60	3.50965106	0.93080346	0.58593610
0.75	0.64	3.28816012	1.09530309	0.58694023

Table 4.11 shows the numerical results of the Skin-friction $f'(0)$, Nusselt number $-\theta'(0)$ and the Sherwood number $-\phi'(0)$ for different values of the Darcy number (Da). As

the Darcy number (Da) increases the Skin-friction coefficient $f'(0)$ and the Sherwood number $-\phi'(0)$ increases, while the Nusselt number $-\theta(0)$ decrease.

Table 4.11: Numerical values of $f'(0)$, $-\theta'(0)$ and $-\phi'(0)$ for different values of (Da).

Da	time(sec)	$f'(0)$	$-\theta'(0)$	$-\phi'(0)$
1.0	0.62	2.98947118	1.26629643	0.58681482
2.0	0.67	3.73335900	1.24275701	0.59676351
3.0	0.62	4.026772776	1.23169437	0.60144550

Table 4.12 shows the numerical results of the Skin-friction $f'(0)$, Nusselt number $-\theta'(0)$ and the Sherwood number $-\phi'(0)$ for different values of the Forchheimer number (Fs). As the Forchheimer number (Fs) increase, the Skin-friction coefficient $f'(0)$ and the Sherwood number $-\phi'(0)$ decreases, whereas the Nusselt number $-\theta'(0)$increases.

Table 4.12: Numerical values of $f'(0)$, $-\theta'(0)$ and $-\phi'(0)$ for different values of (F_s).

F_s	time(sec)	$f'(0)$	$-\theta'(0)$	$-\phi'(0)$
0.0	0.62	3.74438348	1.24172798	0.59719980
0.05	0.62	3.29689167	1.25709562	0.59701052
0.2	0.67	2.29818490	1.28315199	0.57971114

Figure 4.1 illustrates the effect of the thermal Grashof number (Gr) on the velocity profile. The velocity profile increases with an increase in the thermal Grashof number (Gr). The thermal Grashof number (Gr) is the ratio of buoyancy to viscous forces in the boundary layer, thus the increase in the thermal Grashof number (Gr) causes an increase in the bouyancy forces relative to the viscous forces, hence the velocity increase in the boundary layer region.

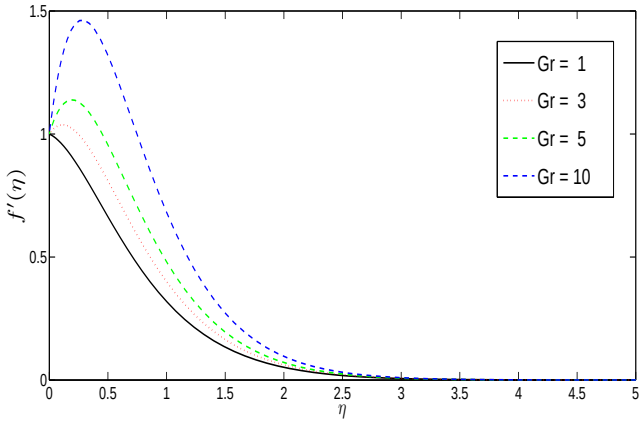

Figure 4.1: Effect of Gr on the velocity profiles

In Figure 4.2, the influence of the modified Grashof number (Gc) is shown. We observe that the modified buoyancy force parameter (Gc) has the same effect on the velocity profile as (Gr), because the buoyancy force is acting like a pressure gradient which accelerates the fluid at the boundary layer region.

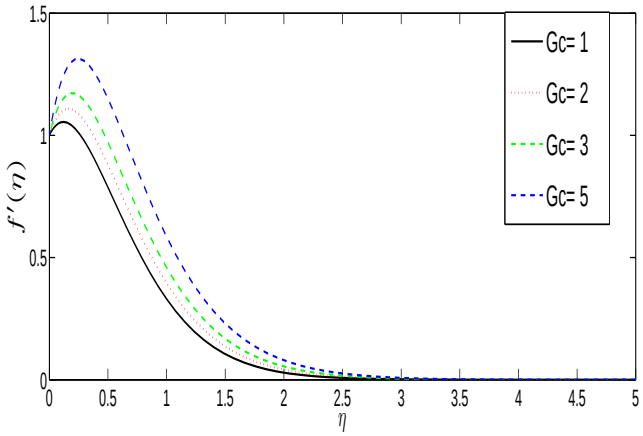

Figure 4.2: Effect of Gc on the velocity profiles

The effect of the magnetic field parameter (M) is shown in Figure 4.3. The velocity profile decreases with an increase in the magnetic field parameter (M). This causes the thinning of the boundary layer thickness. This is because of the application of the magnetic field to an electrically conducting fluid, which produces a resistive type force called Lorentz force. This force is a kind of drag-like force which causes the reduction in the fluid velocity.

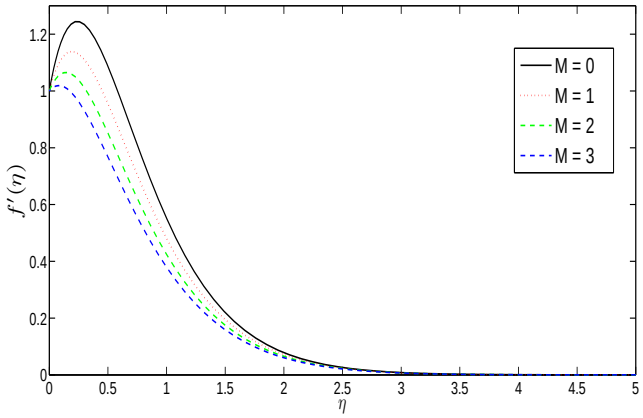

Figure 4.3: Effect of M on the velocity profiles

Figure 4.4 depicts the influence of the Darcy number (Da) on the velocity profile. As it can be seen, an increase of the Darcy number (Da) increases the velocity of the fluid. The increase in the Darcy number (Da) cause an increase in the porosity of the medium causing the fluid to flow quickly.

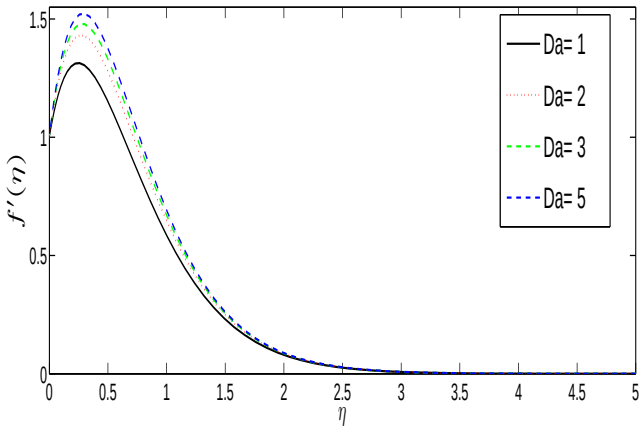

Figure 4.4: Influence of Da on the velocity profiles

Figure 4.5, shows the effect of the Forchheimer number (Fs) on the velocity. It is clearly observed that the velocity of the fluid decreases as the Forchheimer number (Fs) increases. The Forchheimer number (Fs) represent the inertial drag force, therefore increasing the Forchheimer number (Fs) increases the resistance of the flow and cause the decrease in the velocity the fluid.

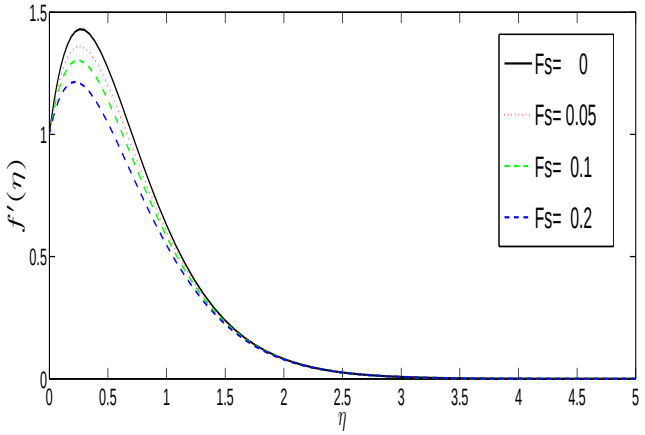

Figure 4.5: Influence of Fs on the velocity profiles

Figures 4.6 and 4.7 illustrates the effects of the Prandtl number (Pr) on the velocity and temperature profiles, respectively. The numerical results show that increasing the Prandtl number (Pr) results in a decrease in the velocity. Hence in Figure 4.7, it can be seen that increasing the Prandtl number (Pr) results in lower temperature of the fluid within the boundary layer because of the decrease of the thermal boundary layer thickness.

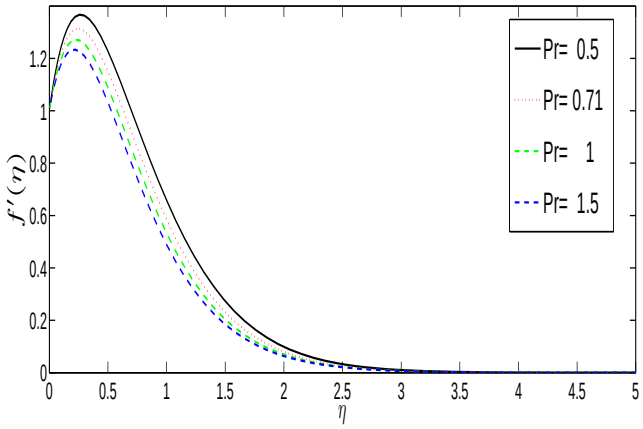

Figure 4.6: Effect of Pr on the velocity profiles

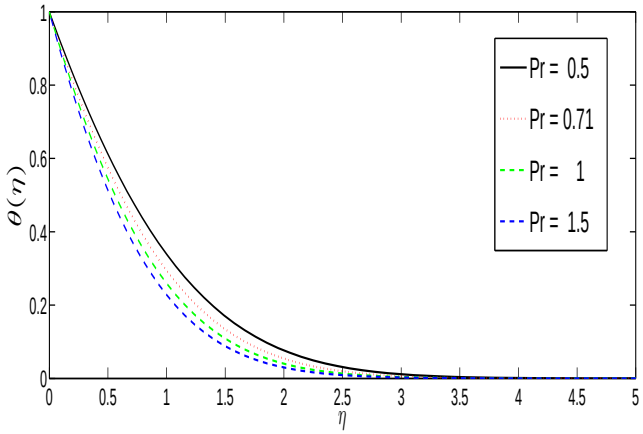

Figure 4.7: Effect of Pr on the temperature profiles

The influence of thermal radiation parameter (R) on velocity and temperature are displayed in Figures 4.8 and 4.9, respectively. We observe that an increase in thermal radiation parameter (R), enhances both the thermal condition of the fluid and the fluid thermal boundary layer. This increase in the temperature causes more flow in the boundary layer causing the velocity of the fluid to increase.

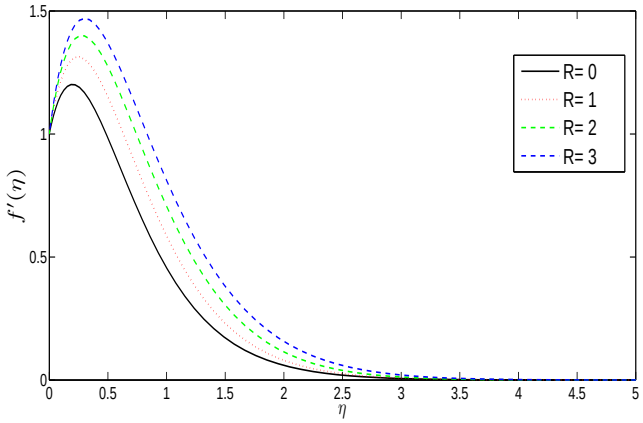

Figure 4.8: Influence of R on the velocity profiles

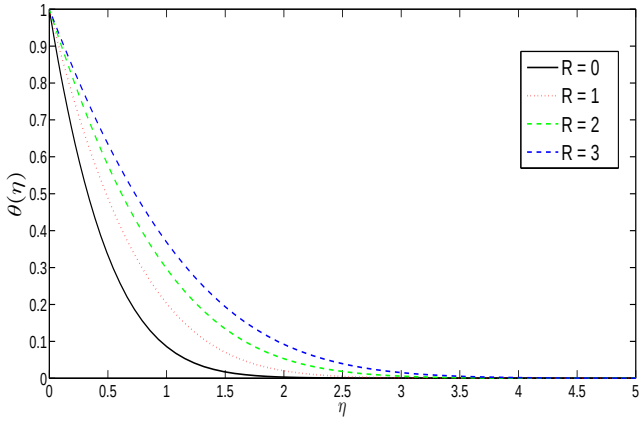

Figure 4.9: Influence of R on the temperature profiles

Figures 4.10 and 4.11, are the plots of velocity and concentration profiles, respectively, for different values of the Schimdt number (Sc). As the Schimdt number (Sc) increases the concentration decrease. This causes the concentration buoyancy effects to decrease resulting in a decrease of the velocity of the fluid. The decrease of velocity and concentration profiles goes together with reduction in the velocity and concentration boundary layers.

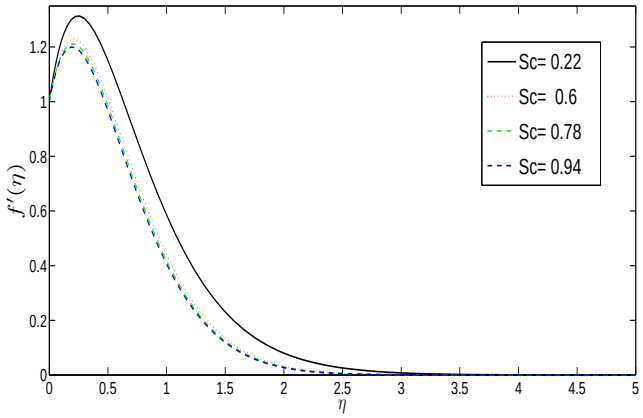

Figure 4.10: Influence of Sc on the velocity profiles

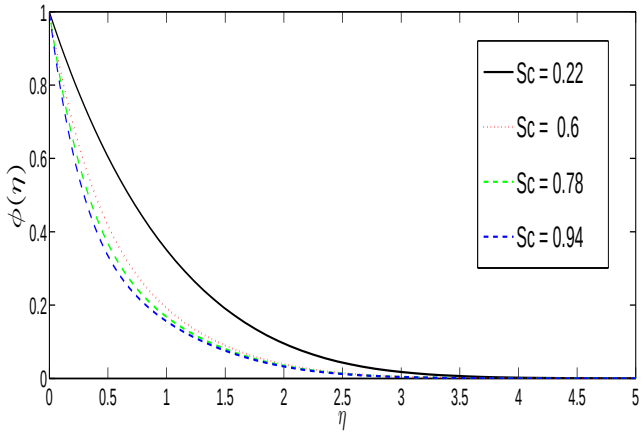

Figure 4.11: Influence of Sc on the concentration profiles

For different values of the chemical reaction parameter (Kr), the velocity and concentration profiles are plotted in Figures 4.12 and 4.13, respectively. It is clearly seen that an increase in the chemical reaction parameter (Kr) results in a decrease in both the velocity and concentration profiles, whereas the temperature of the fluid is not affected with an increase of chemical reaction parameter (Kr). Higher values of (Kr) causes the decrease in the chemical molecular diffusivity, hence the species concentration will be suppressed. Important effect is that the chemical reaction has a tendency to weaken the overshoot in the profiles of the solute concentration in the solutal boundary layer.

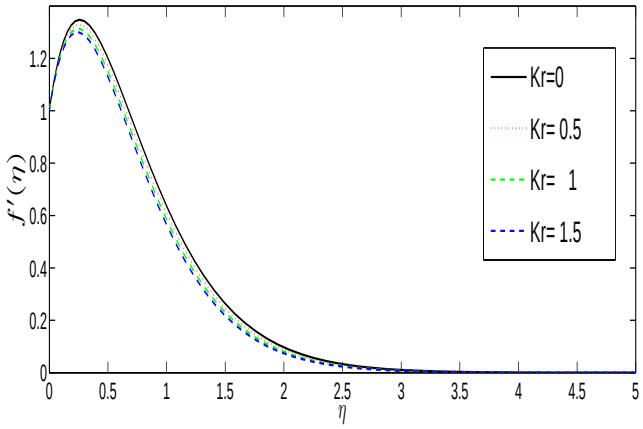

Figure 4.12: Influence of Kr on the velocity profiles

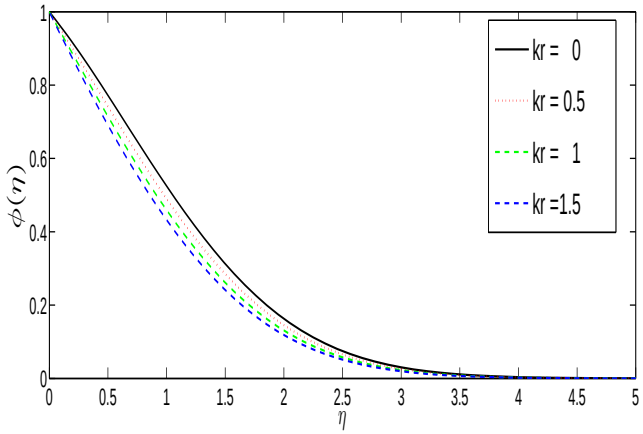

Figure 4.13: Influence of Kr on the concentration profiles

The effect of the suction parameter (c) on the velocity, temperature and concentration of the fluid are shown in Figures 4.14, 4.15 and 4.16, respectively. It is clearly observed that an increase in the suction parameter (c), results in a decrease in velocity, temperature and concentration. This indicates that suction stabilizes the boundary layer.

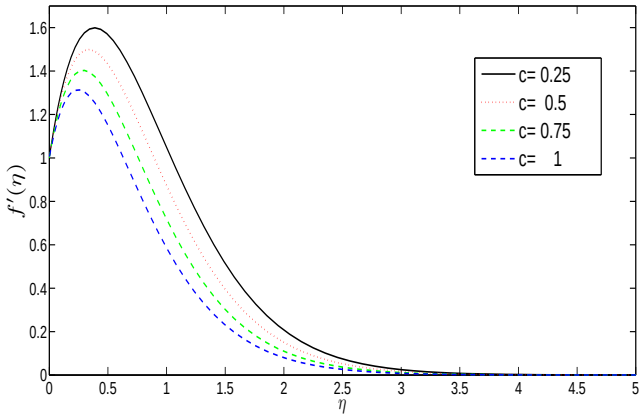

Figure 4.14: Effect of c on the velocity profiles

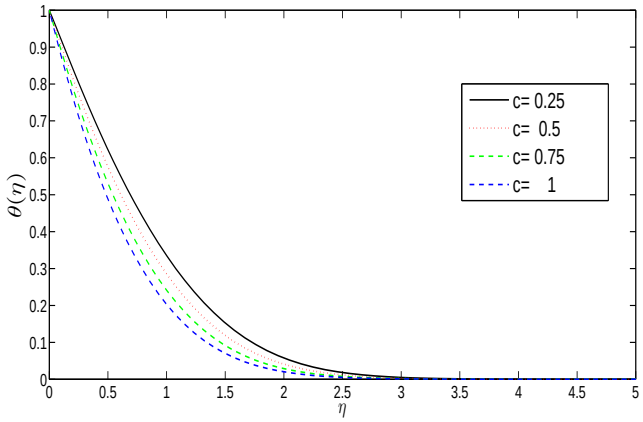

Figure 4.15: Effect of c on the temperature profiles

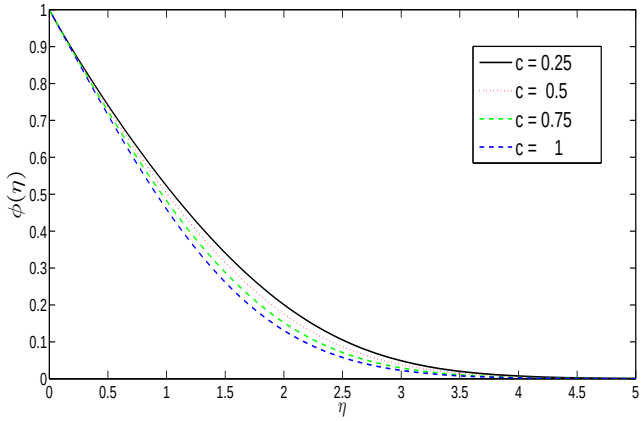

Figure 4.16: Effect of c on the concentration profiles

Figure 4.17 and Figure 4.18, display the effects of the Soret number (Sr) and Dufour number (Du) on the velocity profile, respectively. It is observed that the decrease in Soret number (Sr), results in the decrease in the velocity of the fluid. The velocity profile does not change as the Dufour number (Du) change.

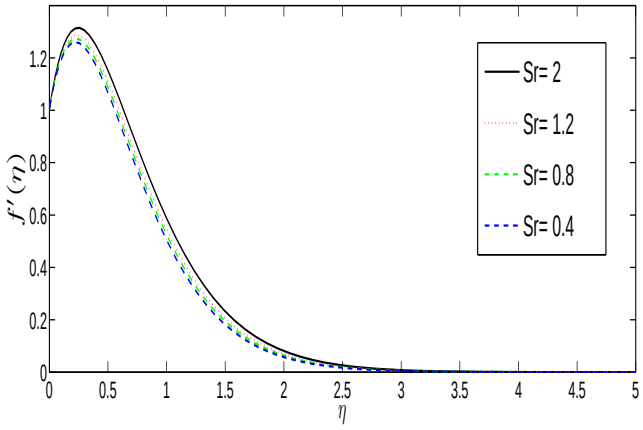

Figure 4.17: Effect of Sr on the velocity profiles

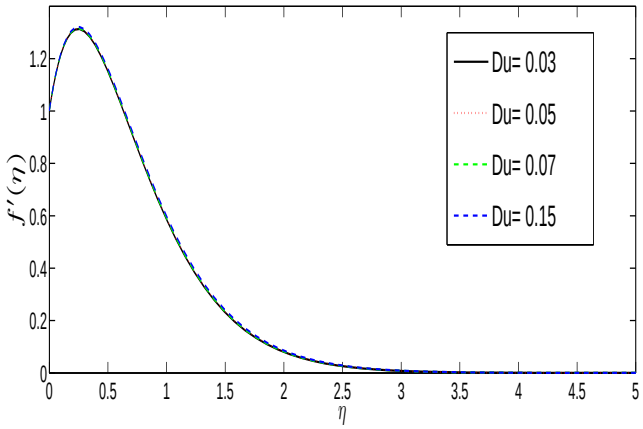

Figure 4.18: Effect of Du on the velocity profiles

The effects of the Soret number (Sr) and Dufour number (Du) on the temperature field are displayed in Figures 4.19 and 4.20, respectively. From these figures we observe that the Soret number (Sr) has insignificant effects on the temperature profile. The temperature profile does not change as the Dufour number (Du) change.

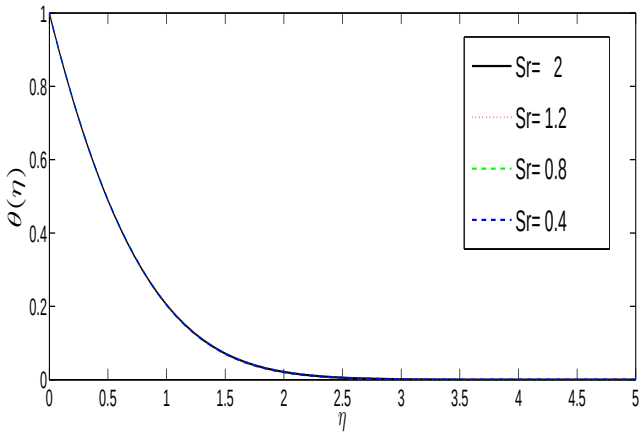

Figure 4.19: Effect of Sr on the temperature profiles

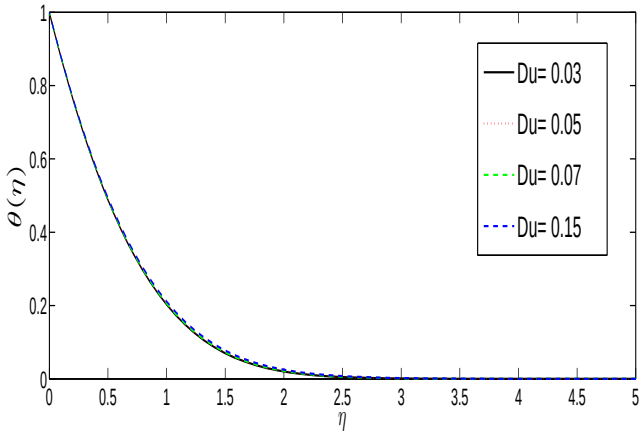

Figure 4.20: Effect of Du on the temperature profiles

The effects of the Soret number (Sr) and Dufour number (Du) on the concentration field are shown in Figures 4.21 and 4.22, respectively. It is noted that the decrease in Soret number (Sr) results in a decrease in the concentration field, whereas the Dufour number (Du) has insignificant effect on the concentration profile.

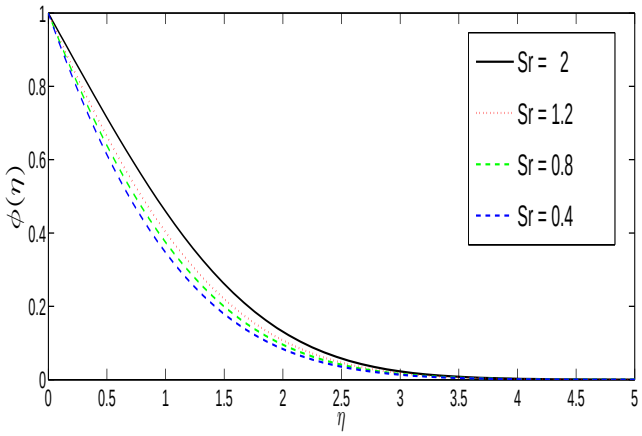

Figure 4.21: Effect of Sr on the Concentration profiles

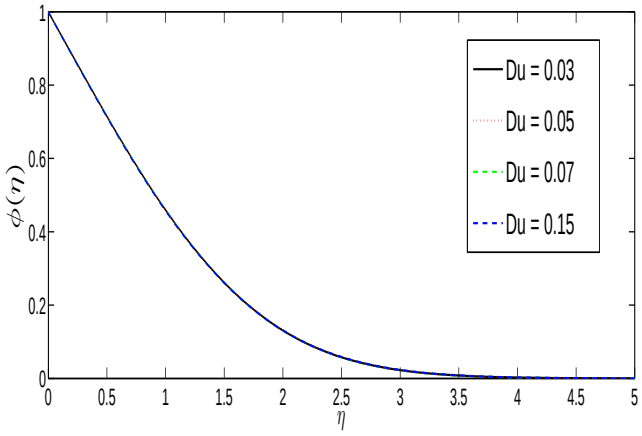

Figure 4.22: Effect of Du on the Concentration profiles

The effects of the viscous dissipation parameter, i.e the Eckert number (Ec) on the velocity, temperature and concentration profiles are displayed in Figures 4.23, 4.24 and 4.25, respectively. We clearly observe that, as the Eckert number (Ec) increase the velocity and temperature profiles also increase, whereas the Eckert number (Ec) does not have significant impact on the concentration profile. The rise in the velocity and temperature profiles is caused by the great viscous dissipative heat. The Eckert number (Ec) is the ratio of the kinetic energy of the flow to the boundary layer enthalpy difference. hence the viscous dissipation effect on the flow is to increase the energy, causing a greater temperature of the fluid and a greater bouyancy force. Therefore the increase in the bouyancy force due to an increase in the dissipation viscousity increases the velocity and

the temperature of the fluild.

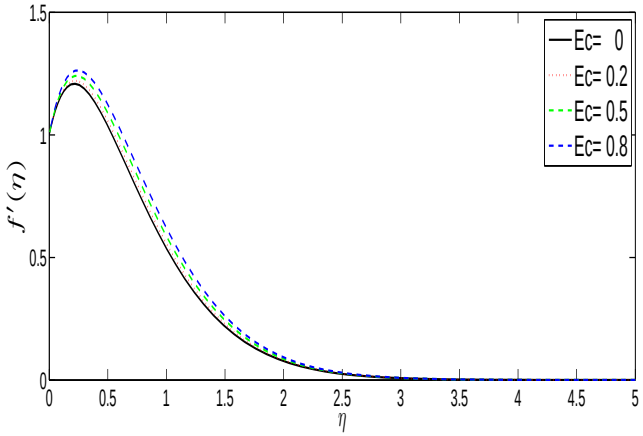

Figure 4.23: Effect of Ec on the velocity profiles

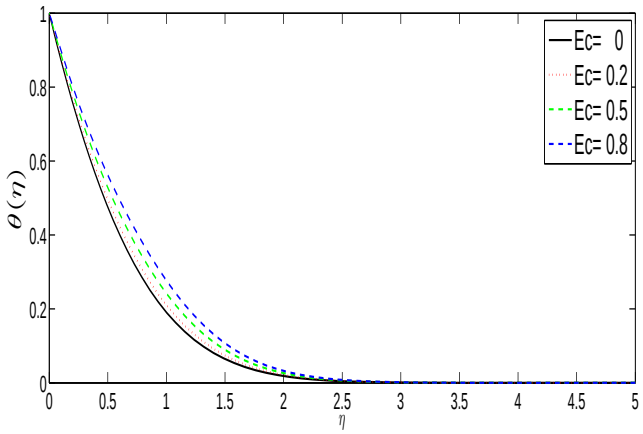

Figure 4.24: Effect of Ec on the temperature profiles

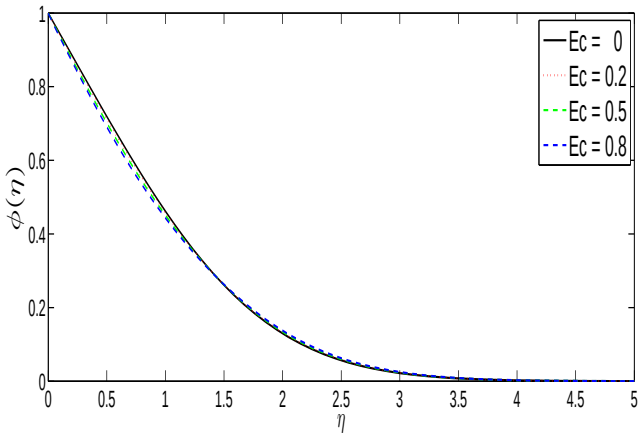

Figure 4.25: Effect of Ec on the Concentration profiles

Chapter 5

Conclusion

In this study, the unsteady MHD mixed convection flow passing over an infinite vertical plate taking into consideration the diffusion-thermo (Dufour) and the thermal-diffusion (Soret) effects with viscous dissipation is numerically analysed. The governing non-linear partial differential equations and their boundary conditions are transformed by a similarity transformation into a system of ordinary differential equations. The non-linear ordinary differential equations are then solved numerically using the Spectral Local Linearization Method (SLLM). The accuracy of this method is validated against the MATLAB in-built `bvp4c` method. The numerical results for the Skin-friction $f'(0)$, the Nusselt number $-\theta'(0)$ and the Sherwood number $-\phi'(0)$, representing the dimensionless velocity, temperature and concentration distributions, respectively, are obtained for various governing parameters. From this study the following conclusions were drawn:

- An excellent agreement was reached between the present results and those obtained using the bvp4c routine, which gives us confidence in our present results.
- Due to strong magnetic field (M) the dimensionless velocity distibution decreases along the flow regime since the magnetic field strength retards the motion of the fluid, while the temperature distribution increases.
- The suction parameter (c) enhances the thermal and concentration boundary layers growth.
- The Prandtl number (Pr) has significant effects on the temperature profiles, while

the velocity and concentration profiles are depressed by increasing the value of the Prandtl number (Pr).

- The increase in the Eckert number (Ec) increases the velocity and temperature profiles and it has insignificant impact on the concentration profile.
- The increase of the thermal Grashof number (Gr) and the modified Grashof number (Gc), increases the velocity profile in the presence of cooling and heating of the plate.
- The concentration components are enhanced as the chemical reaction parameter (Kr) increases, while the velocity components are depressed.
- The velocity profiles increase with an increase in the Darcy number (Da) and the Forchheimer number (Fs).
- It is noted that the Soret number (Sr) and the Dufour number (Du) has negligible effects on temperature profile.
- The decrease in the Soret number (Sr) leads to a decrease in both velocity and concentration of the fluid, while the increase in Dufour number (Du) reduces the velocity and also has negligilbe effect on the concentration profile.

5.1 Recommendations

The SLLM is quick and effective, so we recommend it after comparing our present results with those obtained using Matlab bvp4c technique.

Bibliography

[1] Ahmed S, Joaqun Z and Luis M. L.G, *"Effects of chemical reaction, heat and mass transfer and viscous dissipation over a MHD flow in a vertical porous wall using perturbation method",* International Journal of Heat and Mass Transfer 104 (2017) 409418, www.elsevier.com/locate/ijhmt.

[2] Alam M.S, Rahman M.M and Samad M.A, *"Dufour and Soret effects on unsteady MHD free convective and mass transfer flow past a vertical porous plate in a porous medium",* Nonlinear Analysis: Modelling and control, Vol. 11, no 3, 217-226,2006.

[3] Al-Odat M.Q. and Al-Ghamdi A, *"numerical investigation of Dufour and Soret effects on unsteady MHD natural convection flow past vertical plate embedded in non-Darcy porous medium",* Appl. Math.-Engl. Ed. 33(2), 195-210(2012), DOI 10.1007/s10483-012-1543-9, Shanghai University and Springer-Verlag, Berlin Heidelberg 2012.

[4] Animasaun I.L. , *"Dynamics of unsteady MHD convective flow with thermophoresis of particles and variable thermo-physical properties past a vertical surface moving through binary mixture",* Open Journal of Fluid Dynamics, 2015,5,106-120.

[5] Aruna G, Vijayakumar V.S. and Srinivasa R.R, *"Combined influence of Soret and Dufour effects on unsteady hydromagnetic mixed convective flow in an accelerated vertical wavy plate through a porous medium",* Int.J.Adv.Appl.Math. and Mech. 3(1)(2015)122-134 (ISSN: 2347-2529)

[6] Kendall E.A, *"Numerical analysis"*, Depts of Mathematics and Computer Science, Universityof Iowa, Iowa City, Iowa.

[7] Bhukta D, Dash G.C, Mishra S.R and Baag S, *"Dissipation effect on MHD mixed convection flow over a stretching sheet through porous medium with non-uniform heat source/sink",* Ain Shams Engineering Journal,2090-4479, 2015, http://dx.doi.org/10.1060/ j.asej.2015.08.017.

[8] Bhupendra K.S, Kailash Y, Nidhish K.M and Chaudhary R.C, *"Soret and Dufour effects on unsteady MHD mixed convection flow past a radiative vertical porous plate embedded in a porous medium with chemical reaction",* Applied Mathematics,2012,3,717-723, ,http://dx.doi.org /10.4236/am.2012.37105.

[9] Das M, Mahatha B.K and Nandkeolyar R, *"Mixed cenvection and non-linear radiation in the stagnation point Nanofluid flow towards a stretching sheet with homogeneous heterogeneous reaction effects",* volume 127, 2015, pages 1018-1025, international conference on computational heat and mass transfer.

[10] Gangadhar K. and Suneetha S, *"Soret and Dufour Effects on MHD Free Convection Flow of a Chemically Reacting Fluid Past over a Stretching Sheet with Heat Source/Sink",* Open Science Journal of Mathematics and Application, 2015; 3(5): 136-146, http://www.openscienceonline.com/journal/osjma.

[11] Gadipally D and Murali G, *"Analysis of Soret and Dufour Effects on Unsteady MHD Convective Flow past a Semi-Infinite Vertical Porous Plate via Finite Difference Method",* International Journal of Applied Physics and Mathematics,Volume 4, Number 5, September 2014, doi: 10.7763/IJAPM.2014.V4.306.

[12] Hosseinnia S.M, Mohammad N and Ramin K, *"Numerical study of falling film absorption process in a vertical tube absorber including Soret and Dufour effects",* International Journal of Thermal Sciences 114 (2017) 123e138, www.elsevier.com/locate/ijts.

[13] Mohammed I.S. and Suneetha K, *"Chemical Reaction and Soret Effects on Unsteady MHD Flow of a Viscoelastic Fluid Past an Impulsively Started Infinite Vertical Plate with Heat Source/Sink",* International Journal of Mathematics and Computational Science Vol. 1, No. 1, 2015, pp. 5-14, http://www.publicscienceframework.org/journal/ijmcs.

[14] Ibrahim S.M, Reddy T.S. and Reddy N.B, *"Radiation and chemical reaction effects on MHD convective flow past a moving vertical porous plate",* IJAMAA, vol.7,no.1,(January-June 2012), pp.1-16. Serials publications,ISSN: 0973-3868.

[15] Isah B.Y, Basant K.J and Jeng-Eng L, *"Combined Effects of Thermal Diffusion and Diffusion-Thermo Effects on Transient MHD Natural Convection and Mass Transfer Flow in a Vertical Channel with Thermal Radiation",* Applied Mathematics, 2016, 7, 2354-2373 http://www.scirp.org/journal/am, ISSN Online: 2152-7393, ISSN Print: 2152-7385.

[16] Kalyani C, Reddy C.K and Kishan N, *"MHD Mixed Convection Flow Past a Vertical Porous Plate in a Porous Medium with Heat Source/Sink and Soret Effects",* American Chemical Science Journal 7(3): 150-159, 2015, Article no.ACSj.2015.069 ISSN: 2249-0205, www.sciencedomain.org

[17] Lavanya B and Leela R.A, *"Dufour and soret effects on steady MHD free convective flow past a vertical porous plate embedded in a porous medium with chemical reaction, radiation heat generation and viscous dissipation",* Advances in Applied Science Research, 2014, 5(1):127-142, www.pelagiaresearchlibrary.com

[18] Loganathan P, Iranian D and Ganesan P, *"Dufour and Soret effects on unsteady free convective flow past a semi infinite vertical plate with variable viscosity and thermal conductivity",* International Journal of Engineering and Technology (IJET), Vol 7 No 1 Feb-Mar 2015, ISSN : 0975-4024

[19] Mabood F, Ibrahim S.M, Kumar P.V and Khan W.A, *"Viscous dissipation effects on unsteady mixed convective stagnation point flow using Tiwari-Das nanofluid model",* Results in Physics 7 (2017) 280287, www.journals.elsevier.com/results-in-physics.

[20] Madoda M.M (2012), *"The new Spectral adomian decomposition method and its higher order based iterative schemes for solving highly non-linear two-point boundary value problems.",* PhD. (Chemistry)/ M.Sc (Physics)/ M.A (Philosophy)/ M.com.(Finance) etc.[Unpublished]: University of Johannesburg. Retrieved from: https://ujdigispace.uj.ac.za (Accessed date: 2017/08/10 11:12 am).

[21] Mahender D and Srikanth R.P , *"Unsteady MHD free convection and mass transfer flow past a porous vertical plate in presence of viscous dissipation",* Journal of Physics: Conference Series 662 (2015) 012012 doi:10.1088/1742-6596/662/1/012012

[22] Makinde O.D, *"On MHD mixed convection with soret and dufour effects past a vertical plate embedded in a porous medium",* Latin American Applied Research,41:63-68 (2011).

[23] Makinde O.D and Aziz A, *"MHD mixed convection from a vertical plate embedded in a porous medium with a convective boundary condition",* International Journal of Thermal Sciences, 1290-0729, doi:10.1016/j.ijtherma lsci.2010.05.015.

[24] Mondal H, Dulal l, Sewli C and Sibanda P, *"Thermophoresis and Soret-Dufour on MHD mixed convection mass transfer over an inclined plate with non-uniform heat source/sink and chemical reaction",* Ain Shams Engineering Journal (2017), Ain Shams Engineering Journal, www.sciencedirect.com .

[25] Mortimer R.G AND Eyring H, *" Elementary transition state theory of the Soret and Dufour effects",*Proc. Natl. Acad. Sci. USA Vol. 77, No. 4, pp. 1728-1731, April 1980, Chemistry.

[26] Motsa S.S, *"A new spectral local linearization method for non linear boundary layer flow problems",* Hindawi Publishing Corporation, Journal of Applied Mathematics, Vol. 2013, Article ID 423628, 15 pages,http://dx.doi.org /10.1155/2013/423628.

[27] Motsa S.S, Makukula Z.G and Shateyi S, *"Spectral Local Linearization approach for natural convection boundary layer flow",* Hindawi Publishing Corporation, Mathematical Problems in Engineering, Volume 2013, Article ID 765013, 7 pages, http://dx.doi.org/10.1155/2013/765013.

[28] Mukhopadhyay S and Mandal I.C, *"Magnetohydrodynamic (MHD) mixed convection slip flow and heat transfer over a vertical porous plate",* Engineering Science and Technology, an International Journal,http://dx.doi.org/ 10.1016/ j.jestch.2014.10.001.

[29] Nalinakshi N, Dinesh P.A and Chandrashekhar D.V, *"Soret and Dufour effects on a mixed convection heat and mass transfer with variable fluid properties",* International Journal Of Mathematical Archive-4(11),2013,203-215.

[30] Omowaye A.J, Fagbade A.I and Ajayi A.O, *" Dufour and Soret effects on steady MHD convective flow of a fluid in a porous medium with temperature dependent viscosity: Homotopy analysis approach",* Journal of the Nigerian Mathematical Society (2015), http://dx.doi.org/10.1060/j.jnnms.2015.08.001.

[31] Osalusi E, Jonathan S and Harris R , *"Thermal-diffusion and diffusion-thermo effects on combined heat and mass transfer of a steady MHD convective and slip flow due to a rotating disk with viscous dissipation and Ohmic heating",* International Communications in Heat and Mass Transfer 35 (2008) 908915, www.elsevier.com/locate/ichmt.

[32] Rao J.A, Babu P.R and Raju R.S, *"finite element analysis of unsteady MHD free convection flow past an infinite vertical plate with Soret, Dufour, thermal radiation and heat source",* ARPN Journal of Engineering and Applied Sciences, vol. 10, No. 12, July 2015.

[33] Rashidi M.M, Ali M, Freidoonimehr N, Rostami B and Anwar H.M, *"Mixed convective heat transfer for MHD viscoelastic fluid flow over a porous wedge with thermal radiation",* Hindawi Publishing Corporation, Advances in Mechanical Engineering, Volume 2014, Article ID 735939, 10 pages, http://dx.doi.org/10.1155/2014/735939

[34] Reddy G.V.R, *"Soret and Dufour Effects on MHD free convective flow past a vertical porous plate in the presence of heat generation",* Int. J. of Applied Mechanics and Engineering, 2016, vol.21, No.3, pp.649-665 DOI: 10.1515/ijame-2016-0039.

[35] Shamshuddin M.D and Thirupathi T, *"Soret and Dufour effects on unsteady MHD free convective flow of micropolar fluid with oscillatory plate velocity considering viscous dissipation effects",* Jurnal Teknologi (Sciences and Engineering) 79:4,(2017), 123136.

[36] Shateyi S and Mabood F, *"On a numerical analysis of the MHD mixed convection slip flow near a stagnation point on a non linearly vertical stretching sheet in the presence of viscous dissipation",* October 1, 2015.

[37] Shateyi S and Mabood F, *"On a numerical approach of MHD mixed convection flow, heat and mass transfer of a micropolar fluid over an unsteady stretching sheet with viscous dissipation and thermal radiation",* June 17, 2015.

[38] Shateyi S and Marewo G.T, *"On a new numerical analysis of the hall effect on MHD flow and heat transfer over an unsteady stretching permeable surface in the presence of thermal radiation and heat source/sink",* Boundary Value Problems, a Springer Open Journal, Shateyi and marewo Boundary Value

[39] Srihari K, *"Effects of radiation and soret in the presence of heat source/sink on unsteady MHD flow of a chemically reacting fluid with viscous dissipation",* Department of Mathematics, MGIT, Gandipet, Hyderabad, kotagirisrihari@yahoo.com

[40] Srinivasa R.R, Jithender R.G, Anand R.J, Rashidi M.M, Rama S and Reddy G, *"Analytical and Numerical study of unsteady MHD free convection flow over an exponentially moving vertical plate with Heat Absorption",* International Journal of Thermal Sciences 107 (2016) 303e315, www.elsevier.com/locate/ijts.

[41] Srinivas S, Subramanyam Reddy A, Ramamohan T.R and Anant Kant Shukla, *"Thermal-diffusion and diffusion-thermo effects on MHD flow of viscous fluid between expanding or contracting rotating porous disks with viscous dissipation",* Journal of the Egyptian Mathematical Society (2016) 24, 100107,www.etms-eg.org, www.elsevier.com/locate/joems.

[42] Subhakar M.J and Gangadhar K, *"Soret and Dufour effects on MHD free convection heat and mass transfer flow over a stretching vertical plate with suction and heat source/sink",* International Journal of Modern Engineering Research(IJMER), vol. 2, Issue.5, Sep-Oct.2012 pp-3458-3468, ISSN: 2249-6645.

[43] Suresh, P.H. Veena and V. K. Pravin, *"Numerical investigation of an unsteady mixed convective mass and heat transfer MHD flow with soret effect and viscous dissipation*

in the presence of thermal radiation and heat source/sink", International Journal of Mechanical Engineering and Technology (IJMET), Volume 7, Issue 3, MayJune 2016, pp.170181, Article ID: IJMET 07,03,016.

[44] Uwanta I.J and Usman H, *"On the influence of Soret and Dufour effects on MHD free convective heat and mass transfer flow over a vertical channel with constant suction and viscous dissipation",* Hindawi Publishing Corporation, International Scholarly Research Notices, Volume 2014, Article ID 639159, 11 pages,http://dx.doi.org/10.1155/2014/639159.

[45] Vedavathi N, Ramakrishna K and Jayarami R.K, *"Radiation and mass transfer effects on unsteady MHD convective flow past an infinite vertical plate with Dufour and Soret effects",* Ain Shams Engineering Journal,2090-4479, 2014, http://dx.doi.org/10.1060/j.asej.2014.09.009.

[46] Vempati S.R and Laxmi-Narayana-Gari A.B, *"Soret and Dufour effects on unsteady MHD flow past an infinite vertical porous plate with thermal radiation",* Appl. Math.-Engl. Ed. 31(12), 1481-1496 (2010), DOI 10.1007/s10483-010-1378-9, Shanghai University and Springer-Verlag, Berlin Heidelberg.

[47] Sadeq Z and Sayyed A.F, *"MHD Mixed Convective Flow Past a Vertical Plate Embedded in a Porous Medium with Radiation Effects and Convective Boundary Condition Considering Chemical Reaction",* çankaya University Journal of Science and Engineering Volume 10 (2013), No. 1, 123-136.

[48] https://www.google.co.za/q=unsteady+flow. Date accessed: 09-May-2017

[49] https://en.wikipedia.org/wiki/Magnetohydrodynamics. Date accessed: 09-May-2017

[50] https://www.thermalfluidscentral.org/.Date accessed: 03-July-2017.